Geomorphology 449 (2024) 109067

Contents lists available at ScienceDirect

Geomorphology

journal homepage: www.journals.elsevier.com/geomorphology

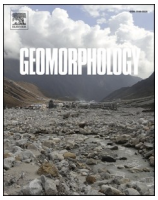

Holocene overbank sedimentation in Central Europe between natural and human drivers - The Weiße Elster River (Central Germany)

Hans von Suchodoletz [a,*], Azra Khosravichenar [a,b], Pierre Fütterer [c], Christoph Zielhofer [a], Birgit Schneider [a], Tobias Sprafke [d,e], Christian Tinapp [f], Alexander Fülling [g], Lukas Werther [h], Harald Stäuble [f], Michael Hein [a], Ulrich Veit [i], Peter Ettel [j], Ulrike Werban [k], Jan Miera [l]

[a] Institute of Geography, Leipzig University, Johannisallee 19a, D-04103 Leipzig, Germany
[b] Institute of Earth System Science and Remote Sensing, Leipzig University, Talstraße 35, D-04103 Leipzig, Germany
[c] Research Area History, Magdeburg University, Zschokkestraße 32, D-39104 Magdeburg, Germany
[d] Land Systems and Sustainable Land Management, Bern University, Hallerstraße 12, CH-3012 Bern, Switzerland
[e] School of Agricultural, Forest and Food Sciences HAFL, Bern University of Applied Sciences BFH, Länggasse 85, CH-3052 Zollikofen, Switzerland
[f] Saxonian Archeological Heritage Office, Zur Wetterwarte 7, D-01109 Dresden, Germany
[g] Sedimentary Geology and Quaternary Research, Freiburg University, Albertstr. 23b, D-79104 Freiburg, Germany
[h] Roman-Germanic Commission, German Archaeological Institute, Palmengartenstraße 10-12, D-60325 Frankfurt/Main, Germany
[i] Historical Seminar, Leipzig University, Ritterstraße 14, D-04109 Leipzig, Germany
[j] Seminar for Prehistoric and Early Archeology, Jena University, Löbdergraben 24a, D-07743 Jena, Germany
[k] Department of Monitoring and Exploration Technologies, Helmholtz Centre for Environmental Research - UFZ Leipzig, Permoserstraße 15, D-04318 Leipzig, Germany
[l] Historical Seminar, Münster University, Domplatz 20-22, D-48143 Münster, Germany

ARTICLE INFO

Keywords:
Fluvial geomorphology
Overbank deposition
Central Europe
Settlement activity
Climate changes
Landscape sensitivity
Holocene

ABSTRACT

Up to several meters thick fine-grained Holocene overbank deposits are ubiquitously found in most Western and Central European lowland floodplains. However, despite their large importance for the geomorphological and geoecological floodplain properties, the interplay of different possible causes for their formation are not well understood yet. Most authors suggest human-induced deforestation as the main precondition for sediment mobilization and transport from the slopes to the floodplain, whereas others suggest a stronger influence of climatic factors. This current research gap is caused by often missing well-resolved fluvial chronostratigraphies and spatio-temporal information about former human activity within the studied catchments. To fill this gap we exemplarily studied Holocene overbank sedimentation and possible human or natural drivers in the meso-scale Weiße Elster catchment in Central Germany. To do so, we applied numerical dating as well as sedimentological and micromorphological analyses to Holocene fluvial sediments along three floodplain transects. Furthermore, we built up an unprecedented systematic spatio-temporal database of former human activity within the catchment from the Neolithic until the Early Modern Ages. Together with published paleoclimatic data, this database allowed an unprecedented, systematic comparison of Holocene overbank sedimentation phases with possible external controls. Our data show that some overbank sedimentation phases were directly linked with human activities in the affected site sub-catchments, whereas others were not. Instead, all phases seemed to be linked with natural factors. This difference with most former studies could possibly be explained by previously often limited numerical dating of the fluvial sediments and by largely missing spatio-temporally well-resolved regional settlement records, hindering a precise temporal link of fluvial sedimentation with former human settlement. Furthermore, this difference could possibly also be explained by a relatively high natural sensitivity of the landscape dynamics in the Central German lowlands, showing a subcontinental climate, towards climatic external controls.

* Corresponding author.
E-mail address: hans.von.suchodoletz@uni-leipzig.de (H. von Suchodoletz).

https://doi.org/10.1016/j.geomorph.2024.109067
Received 10 November 2023; Received in revised form 23 December 2023; Accepted 10 January 2024
Available online 16 January 2024

1. Introduction

Up to several meters thick Holocene fine-grained overbank deposits consisting of sand, silt and clay (Brown et al., 2018) are ubiquitously found in most Western and Central European lowland floodplains (Macklin and Lewin, 1993; Starkel et al., 2006; Hoffmann et al., 2007; Hürkamp et al., 2009; Notebaert et al., 2011; Fuchs et al., 2011; Houben et al., 2013; Gebica et al., 2016; Kirchner et al., 2022). Their deposition strongly changed the geomorphological and geoecological floodplain properties, since prior to their deposition (i) the valley floors were largely dominated by thin fine-grained organic-rich sediments or peat deposits (Rittweger, 2000; Broothaerts et al., 2014a; Brown et al., 2018), (ii) the channel patterns were braided or anabranching/anastomosing and not meandering as today (Notebaert et al., 2018; Brown et al., 2018), and (iii) due to a higher flood risk and relatively higher groundwater table caused by their lower elevation above the river channel floodplains often were less suitable for human activities (Lespez et al., 2013; Tinapp et al., 2019). Furthermore, Holocene overbank deposits form important storages for organic carbon (Sutfin et al., 2016; Swinnen et al., 2020) and pollutants (Hürkamp et al., 2009; Buchty-Lemke et al., 2019). However, despite their large importance for the geomorphological and geoecological floodplain properties, the interplay of different possible causes of Holocene overbank deposition is currently not fully understood: Whereas most authors suggest human-induced deforestation as the main precondition to allow sediment mobilization and transport from the slopes to the floodplains (Starkel et al., 2006; Tinapp et al., 2008; Hürkamp et al., 2009; Fuchs et al., 2011; Notebaert et al., 2011; Houben et al., 2013; Stolz et al., 2013), also based on individual pre-Neolithic fine-grained floodplain deposits others suggest a stronger influence of climatic factors (Lüttig, 1960; Lespez et al., 2008; Gebica et al., 2016; Kirchner et al., 2022). On the one hand, this current research gap is caused by often missing well-resolved fluvial chronostratigraphies. On the other hand, apart from singular studies (Broothaerts et al., 2014b; Kirchner et al., 2022) well-resolved spatio-temporal information about former human activity within the studied catchments is largely missing.

The floodplain of the meso-scale Weiße Elster River in Central Germany is well suited to systematically address this research question: (i) Its catchment is mostly covered by loess and loess sediments, causing a high susceptibility towards external human or climatic disturbances (Haase et al., 2007; Wolf and Faust, 2013), (ii) Its catchment has been settled since the Early Neolithic, showing a long history of human occupation (Tinapp and Stäuble, 2000; Miera et al., 2022), and (iii) unlike many other Western and Central European Holocene floodplains with overbank aggradation only starting about 4–2 ka (Niller, 1998; Fuchs et al., 2011; Houben et al., 2013; Stolz et al., 2013; Notebaert et al., 2018), significant amounts of such fine-grained sediments were already deposited since about 7–5 ka (Litt et al., 1987; Fuhrmann, 1999, 2005; Tinapp, 2003). However, most former studies in the Weiße Elster river system investigated only single isolated sites instead of multiple floodplain cross-sections. Furthermore, they largely lacked highly resolved and precise age control, and mostly also well-resolved spatio-temporal information about former human activity in the catchments (Neumeister, 1964; Händel, 1967; Fuhrmann, 1999, 2005; Tinapp, 2003; Tinapp et al., 2008, 2019). Therefore, also for the Weiße Elster river system the human and natural causes for overbank deposition are controversially discussed (Fuhrmann, 1999, 2005; Tinapp, 2003; Tinapp et al., 2008).

The main goal of this study was to investigate the evolution of Holocene overbank sedimentation and possible human or natural drivers in the Weiße Elster floodplain. To study Holocene overbank deposition, we applied numerical dating as well as sedimentological and micromorphological analyses to fluvial sediments along three floodplain transects in the middle Weiße Elster floodplain. The fluvial architecture along these transects was previously studied using geophysical and stratigraphical methods (von Suchodoletz et al., 2022). Furthermore, using published and unpublished archaeological and historic data, in continuation of Miera et al. (2022) we built up a systematic spatio-temporal database of former human activity within the catchment from the Neolithic until the Early Modern Age. Together with published paleoclimatic data, this comprehensive database allows an unprecedented, systematic comparison of Holocene overbank deposition phases with possible external controls.

2. Study area and studied floodplain sites

2.1. Study area

The 245 km long Weiße Elster River in Central Germany with a catchment of 5154 km^2 originates from the Central European Uplands in the NW Czech Republic at an altitude of about 810 m above sea level, and flows into the Saale River that drains via the Elbe River into the North Sea (Fig. 1a). During the first 120 km the river flows through Pre-Permian rocks (SLUG, 1992), and the valley shows deep gorges interchanging with small local floodplains. Further downstream, a continuous few hundred meters up to one kilometer wide floodplain first cut into Lopingian to Lower Triassic rocks is formed, extending up to the confluence with the Saale River (Händel, 1969). North of Zeitz the valley widens to about two kilometers and is developed in mostly Quaternary loose sediments (SLUG, 1992). In the Altenburg-Zeitz Loess Hill Area (BFN, 2012), these materials are covered by up to several meters thick loess thinning out southwards, and changing northwards into thin sand loess and drift sand (Eissmann, 2002) (Fig. 1b).

According to the Köppen-Geiger classification the Weiße Elster river catchment shows a sub-continental Cfb climate (Kottek et al., 2006): Maximum annual precipitation of up to 1000 mm in the southeastern catchment contrasts with amounts of <700 mm/a in the remaining parts. Mean discharge is peaking during spring due to snowmelt, but most extreme flooding during summer is linked with convective and Vb weather types (Nissen et al., 2013) (Fig. 1c). The potential natural vegetation ranges from *Fagus* and mixed *Fagus* forests in the upper to *Quercus-Carpinus* forests in the lower catchment (Bohn and Welß, 2003). Especially along the middle and lower river course most forests were replaced by agricultural fields, and within the upper catchment artificial coniferous forests dominate today. Settlement activities in the northern catchment started during the Early Neolithic about 7.5 ka. Subsequently the settlement activity varied in space and time, showing periods of intensive settlement such as during the Early and Late Neolithic or Late Bronze Period, whereas finds from the Middle Neolithic, Middle Bronze or Migration Period are rather rare. Since the Middle Ages the catchment was mostly continuously settled (Tinapp and Stäuble, 2000; Heynowski and Reiß, 2010; Fütterer, 2016; Miera et al., 2022).

2.2. Studied floodplain sites

In a previous study, we investigated the fluvial architecture at three sites in the middle Weiße Elster floodplain (von Suchodoletz et al., 2022). During this study, we revisited these sites for further investigations:

2.2.1. Salsitz (Fig. 2a)

The ca. 1 km wide floodplain near Salsitz with a catchment of about 2430 km^2 is surrounded by hill slopes with relative elevations between 70 and 100 m. These consist of Lower Triassic sand-, silt- and claystones, which are covered by up to >2 m thick loess (KPGL, 1908). The floodplain shows three main morphological Holocene lateral terrace levels with maximal elevation differences of about 2 m (also called 'paleomeander terraces'; Schirmer, 1995, Erkens et al., 2009), and beyond the eastern main river channel, a secondary channel exists in the central floodplain at least since 1748 CE. Several dry valleys and creeks, descending from the surrounding hills, form partly eroded alluvial fans at their transitions into the floodplain. We formerly studied the fluvial

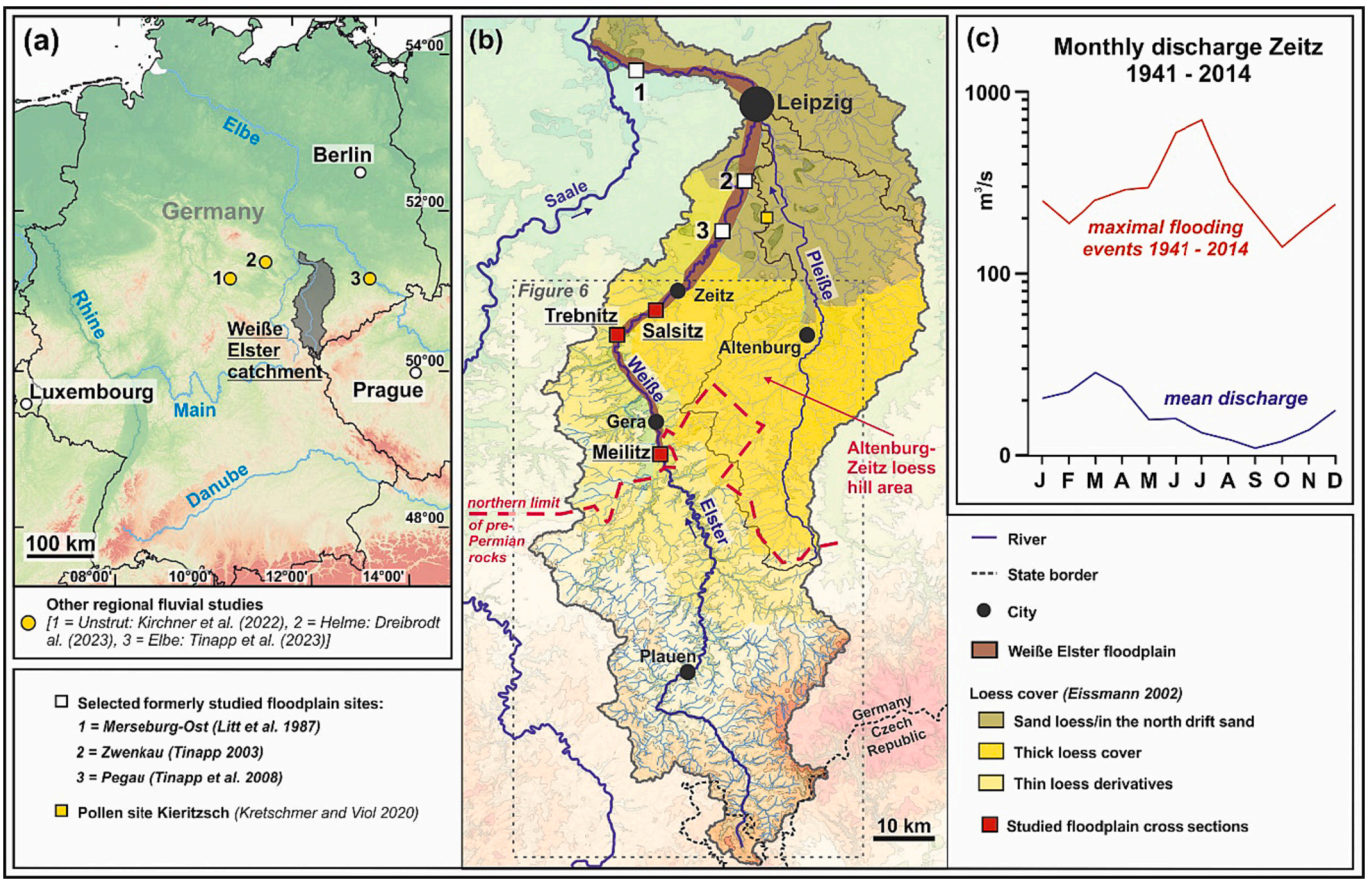

Fig. 1. (a) Location of the Weiße Elster catchment in Central Germany, (b) the Weiße Elster catchment. Highlighted are the floodplain area, the loess cover, current and former floodplain study sites, pollen site Kieritzsch (Kretschmer and Viol, 2020), the Altenburg-Zeitz Loess Hill Area (BFN, 2012) and the northern limit of Pre-Permian rocks (SLUG, 1992), (c) monthly discharge values of the station Zeitz 1941–2014 (location see Fig. b) (www.hochwasservorhersage.sachsen-anhalt.de).

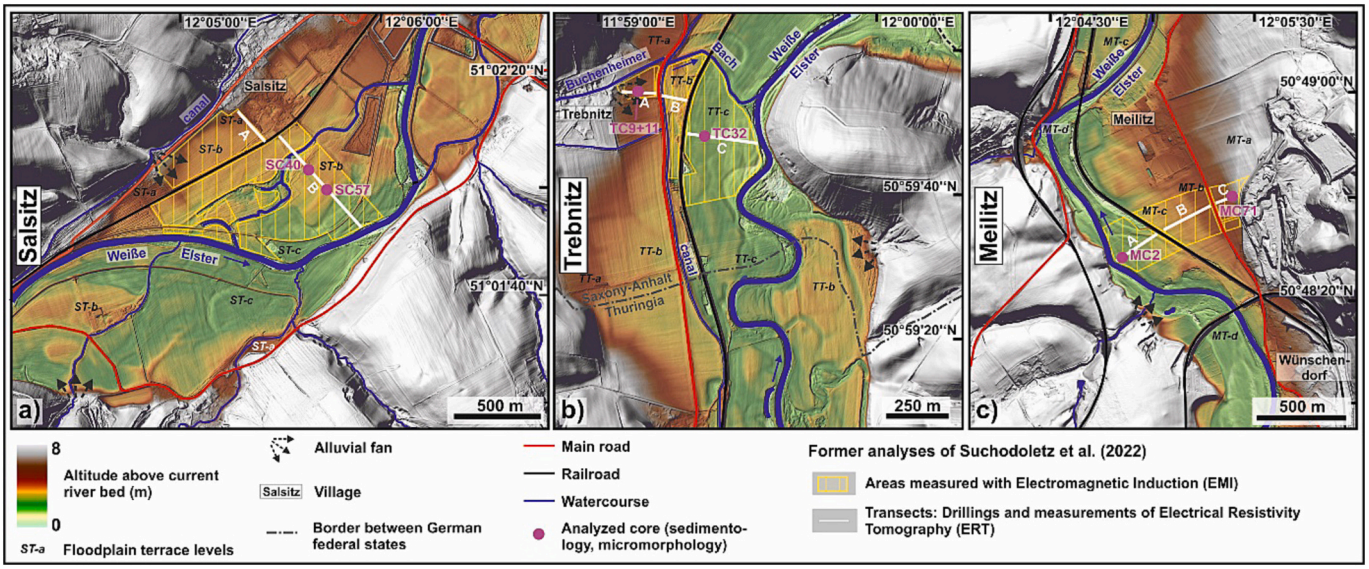

Fig. 2. The sites in the Weiße Elster floodplain that were investigated during this study, including the positions of cores that were sedimentologically and/or micromorphologically analyzed. Furthermore, the locations of the transects and areas studied by von Suchodoletz et al. (2022) to investigate the local fluvial architecture are shown: (a) Salsitz, (b) Trebnitz, (c) Meilitz.

architecture along a 950 m long floodplain transect using electrical resistivity (ERT) measurements and 81 drill cores, and a surrounding area of about 75 ha using electrical magnetic induction (EMI) measurements. These investigations suggested three main Holocene sediment generations in this part of the floodplain that were separated from each other by two large lateral erosion periods.

2.2.2. Trebnitz (Fig. 2b)

The ca. 600 m wide floodplain near Trebnitz with a catchment of about 2340 km^2 is surrounded by hill slopes with relative elevations between 70 and 130 m. They consist of Lower Triassic sand-, silt and claystones, covered with Elsterian glacial deposits on the lower and a thin loess cover on the upper slopes (KPG, 1852; TLB, 1993). The floodplain shows three main Holocene lateral terrace levels with maximal elevation differences of about 2.5 m, and the river flows in a meandering single-thread channel today. Some dry valleys descend from the surrounding slopes, showing at some places small alluvial fans at their transitions into the floodplain. Furthermore, a tributary creek enters the floodplain from the west (Buchenheimer Bach), and has aggraded a small alluvial fan on which the village Trebnitz was built. We formerly studied the fluvial architecture along a 550 m long floodplain transect using ERT measurements and 50 drill cores, and a surrounding area of about 21 ha using EMI measurements. These investigations suggested three main Holocene sediment generations in this part of the floodplain that were separated from each other by two large lateral erosion periods.

2.2.3. Meilitz (Fig. 2c)

The ca. 800 m wide floodplain near Meilitz, located in the most upstream part of the continuous floodplain extending down to the confluence of Elster and Saale River, has a catchment of about 1930 km^2. The surrounding hill slopes show relative elevations between 100 and 130 m, and consist of Lower Triassic sand-, silt and claystones and Lopingian carbonates and silt-claystones (KPGL, 1892, 1912). The floodplain shows four main Holocene lateral terrace levels with maximal elevation differences of about 1.3 m, and the river flows in one channel today. Some dry valleys descend from the surrounding slopes that in some places show small alluvial fans upon entering the floodplain, and a small tributary stream converges from the west. We formerly studied the fluvial architecture along a 710 m long floodplain transect using ERT measurements and 75 drill cores, and a surrounding area of about 26 ha using EMI measurements. These investigations suggested two main Holocene sediment generations in this part of the floodplain that were separated from each other by one large lateral erosion period.

3. Methods

3.1. Chronology

From all three transects we took sediment samples from selected cores for luminescence dating, and organic material from transects Trebnitz and Meilitz for radiocarbon dating. Together with the previous radiocarbon ages from the transect of Salsitz of Ballasus et al. (2022a), high-resolution chronostratigraphies of the transects could be established.

3.1.1. Radiocarbon dating

17 organic samples (charcoal, peat with plant remains, soil matrix; Table 1) were dated in the radiocarbon dating laboratory of the CEZ Mannheim. The soil samples were prepared with the Acid-Base-Acid method (Steinhof et al., 2017), and the bulk organic matter after

Table 1
List of radiocarbon ages, and results of radiocarbon dating. The ages are ordered from west to east and from top to bottom.

Lab number	Core and sample depth [cm]	Material	Sedimentary context	$\delta^{13}C$ [‰]	^{14}C age [years BP]	Calibrated ^{14}C age [cal. years BP, 2 sigma error]
Trebnitz						
MAMS-37770	TC2, 487	Peat with plant remains	Uppermost part of peat layer	−12.0	8405 ± 31	9526–9311
MAMS-37769	TC8, 332	Charcoal	Overbank deposit	−31.4	8401 ± 47	9528–9297
MAMS-37767	TC9, 121	Charcoal	Overbank deposit	−30.4	3440 ± 30	3828–3581
MAMS-37768	TC9, 170	Charcoal	Gravelly overbank deposit	−30.2	4504 ± 37	*5308–4989**
MAMS-37765	TC 10, 59	Charcoal	Overbank deposit	−27.2	1445 ± 23	*1368–1300**
MAMS-46724	TC11, 186-190	Soil matrix	Black Floodplain Soil	−34.6	5917 ± 24	6789–6675
MAMS-46726	TC11, 194-198	Soil matrix	Black Floodplain Soil	−32.4	6437 ± 30	7425–7282
MAMS-61440	TC11, 214-218	Soil matrix	Black Floodplain Soil	−31.9	7227 ± 27	8170–7966
MAMS-43193	TC12, 48	Charcoal	Overbank deposit	−34.1	340 ± 18	471–315
MAMS-43191	TC13, 137	Charcoal	Transition between Black Floodplain Soil and overbank deposit	−22.3	3825 ± 20	4348–4102
MAMS-43192	TC13, 248	Charcoal	Overbank deposit	−30.7	8561 ± 27	*9550–9487**
MAMS-43190	TC14, 140	Charcoal	Gravelly overbank deposit	−43.1	3713 ± 28	4150–3976
MAMS-37771	TC29, 121	Charcoal	Overbank deposit	−35.5	1044 ± 23	*1047–918**
MAMS-37772	TC32, 45	Charcoal	Overbank deposit	−35.9	1504 ± 22	*1409–1315**
MAMS-37773	TC33, 136	Charcoal	Overbank deposit	−33.3	2325 ± 30	*2421–2181**
Meilitz						
MAMS-61438	MC74, 158	Charcoal	Overbank deposit	−35.7	5817 ± 27	6731–6503
MAMS-61439	MC74, 295	Charcoal	Abandoned inorganic channel fill	−24.9	9099 ± 29	10,363–10,198

Please note: Based on their stratigraphic context, some radiocarbon ages obviously represent re-deposited charcoal samples (marked with *). These ages are not included into the age model. For more detailed explanation see text.

removing soluble humic acids was dated. The ages were calibrated using the software SwissCal and the Intcal20 calibration curve (Reimer et al., 2020).

3.1.2. Luminescence dating

41 luminescence samples were taken using light-proof plastic inliners (Table 2), which were opened under subdued red light in the luminescence preparation laboratory at Leipzig University. Next to sieving, sample preparation to obtain the grain size fraction 90–200 μm included 10 and 37 % HCl and 10 and 30 % H_2O_2 treatment to remove carbonate and organic matter, respectively. Subsequently, from most samples quartz was obtained by removing heavy minerals ($\sigma > 2.75$ g/cm^3) and feldspars ($\sigma < 2.62$ g/cm^3) using sodium metatungstate-monohydrate. Then, the obtained quartz fraction was etched with 40 % HF for ca. 45 min to remove any remaining feldspar and the α-irradiated outer rim of the grains. This was followed by sieving with 63 μm mesh width, in order to obtain as much datable material as possible given the partly low material output from the plastic inliners. Given that not enough quartz fine sand was available in samples OSL-E-21 and OSL-E-33, for these samples the polymineral fraction 4–11 μm was obtained in Atterberg settling tubes using Stoke's Law. The paleodoses were measured in the luminescence laboratory of the University of Freiburg/Breisgau on an updated Risø TL/OSL-DA-15 C/D reader (quartz coarse grain) and a Freiberg Instruments LexsygStandard device (polymineral fine grain). Quartz coarse grain samples were mounted on stainless steel cups (small aliquots of 2 mm) using silicone oil, and polymineral fine grain aliquots were prepared by pipetting a suspension of fine grains and distilled water (1.5 mg/aliquot) using stainless steel cups. Quartz coarse grain was measured with a modified OSL SAR protocol (Murray and Wintle, 2000), including a preheat of 200 °C (10 s), a test dose cutheat of 180 °C using blue light stimulation (470 nm), and determination of the OSL IR depletion ratio according to Duller (2003). The OSL signals were detected through a Hoya U-340 filter (340 nm). Polymineral fine grain was measured applying a post-IR IRSL SAR protocol (Buylaert et al., 2009), including an IR stimulation (870 nm) at 50 °C followed by a second IRSL measurement at 225 °C, and the IRSL signal was detected using a Schott BG-39 and AHF-BrightLine HC 414/46-Interference filter (410 nm). The high-temperature IRSL signal is considered as more stable and less affected by anomalous fading as the conventional signal at 50 °C, and was hence used for further analysis. Preheat was performed at 250 °C for 60 s, and a hotbleach of 290 °C for 40 s after the readout of the post IR IRSL test dose signals. All preheat procedures were confirmed in dose recovery tests. Possible residual doses were neither determined nor subtracted from the post-IR IRSL measurement results nor fading correction was performed, since both post-IR IRSL ages (samples OSL-E-21, 33) are certainly strongly overestimated (Table 2) so that time-consuming fading measurements would have made no sense. Hence, these ages represent maximum ages. De calculation for the fine-grained polymineral samples was performed using the Central Age Model (Galbraith et al., 1999). For the coarse quartz grain samples, due to a large scatter of the equivalent doses (De's) indicating incomplete bleaching during last sediment transport, we calculated the De's from the lower parts of the De-distributions based on the minimum age model (Galbraith et al., 1999).

The dose rate was measured using low-level gamma-spectrometry at the "Labor für Umwelt- und Radionuklidanalytik (Niederniveaumesslabor Felsenkeller)" of VKTA Rossendorf (Germany). Due to probably strongly fluctuating groundwater levels in the floodplain, the measured *in-situ* water contents cannot be regarded as reliable. Hence, for loamy-sandy samples we used a value of 10 ± 10 % and for loamy-clayey samples of 20 ± 10 %, what should encompass the average water contents throughout the burial periods (Fuchs, 2001).

3.2. Sediment properties

To better characterize sediment and paleosol properties, we retrieved selected cores using percussion drilling (Atlas Copco Cobra Pro hammer) and a 60 mm-diameter open corer. These cores were sampled for sedimentological and micromorphological analyses (core positions see Figs. 2, 3). Some data of core SC40 were formerly published in Ballasus et al. (2022b).

Carbonate contents were measured according to Scheibler in an Eijkelkamp Calcimeter apparatus, i.e., based on the CO_2-volume produced during the reaction of the sediments with 10 % HCl.

Total organic carbon (TOC) contents were determined by measuring C_{total} with a Vario EL cube elemental analyser, and subsequently subtracting inorganic carbon (taken from carbonate measurements) from C_{total}.

To determine *element contents* using a Spectro Xepos eX-ray fluorescence spectrometer, air dried sample material was ground in a vibratory mill for 10 min to obtain the required grain size <30 μm and homogenisation. Prior to measurement, a 32 mm-pellet was produced by mixing and pressing 8 g of the ground material with 2 g CEREOX Licowax. To identify the weathering degree of the sediments we applied the ratio Rb/Sr, with high ratios indicating intensive weathering since the smaller Sr^{2+}-ion is more easily discharged during weathering than the larger Rb^{+}-ion (Tinapp et al., 2023). Furthermore, Rb is fixed to clay minerals, whereas Sr is leached by flowing water (McLennan et al., 1993).

Grain size analyses were performed using 10 g of bulk sample material. After destroying organic matter with 35 % H_2O_2, the samples were dispersed in 10 ml 0.4 N sodium pyrophosphate solution ($Na_4P_2O_7$) followed by ultrasonic treatment for 45 min. Sand contents (63–2000 μm) were determined by dry sieving. The material <63 μm was measured with X-ray granulometry (XRG) using a SediGraph III 5120 (Micromeritics).

Mass-specific magnetic susceptibility was measured using a Bartington MS3 magnetic susceptibility meter equipped with a MS2B dual frequency sensor. After softly grounding and densely packing the material into plastic boxes, volumetric magnetic susceptibility was measured with a frequency of 0.465 kHz and normalized with the sample mass.

The above-described analyses were carried out in the laboratory of the Geographical Institute of Leipzig University/Germany.

For micromorphological analyses, oriented undisturbed soil samples were taken from cores SC40 (Salsitz) and TC9 (Trebnitz) (locations see Fig. 3). After air-drying and impregnating with Oldopal P 80-21, hardened blocks were cut and sliced into 50 * 50 mm thin sections. Thin sections were described under a polarizing light microscope, using the terminology of Stoops (2003). Semi-quantitative analysis of features followed Sprafke (2016), with an adapted list of parameters. The description of the thin sections was carried out at the Institute of Geology at Bern University/Switzerland.

3.3. Former settlement activity

The origin of the floodplain sediments from the middle reach of the Weiße Elster River is still debated, i.e., it is not clear whether they largely originate from the upper catchment or from the surroundings of the studied sites (Ballasus et al., 2022a; Matys-Grygar, 2022; Zielhofer, 2022). Hence, we will discuss our data from the studied floodplain transects in the context of both the total and smaller local site subcatchments.

3.3.1. Recording and pre-processing of archaeological data

To study prehistoric and Medieval settlement in our study area, we built up an archaeological database based on archaeological publications and local area files (German: Ortsakten) from the Saxonian Archaeological Heritage Office, State Office for Preservation of Monuments and Archaeology Saxony-Anhalt, and Thuringian State Office for Heritage Management and Archaeology. The archaeological sites were standardized to provide a systematically structured database, and to enable comparability with future studies (for more details see Miera et al., 2022):

Table 2
List of luminescence samples, and analytical results of luminescence dating.

Lab number	Core and sample depth [cm]	U max./min.[1] [Bq/kg]	Th [Bq/kg]	K [Bq/kg]	Assumed water content [%]	Total dose rate max./min.[1] [Gy/ka]	Cosmic dose rate [Gy/ka]	Measurement technique[2] *(Sigma b[3])*	Equivalent dose [Gy]	Age min./max[1] *(resulting max. age range[4])* [ka]	Possible cause of over-/underestimation[6]
Salsitz											
OSL-E-1	SC25, 38-48	52 ± 6/37 ± 5	56 ± 4	660 ± 70	10 ± 10	3.80 ± 0.63/3.55 ± 0.59	0.20 ± 0.02	CG *(0.14)*	2.23 ± 0.35	0.59 ± 0.10/0.63 ± 0.11 *(0.49–0.74)*[b]	–
OSL-E-2	SC25, 82-92	76 ± 7/46 ± 5	62 ± 4	760 ± 80	20 ± 10	4.16 ± 0.26/3.69 ± 0.24	0.19 ± 0.02	CG *(0.14)*	~14.5[5]	3.49–3.92[5,b]	–
OSL-E-12	SC39, 95-105	56 ± 5	55 ± 3	730 ± 50	15 ± 10	3.85 ± 0.41	0.19 ± 0.02	CG *(0.14)*	10.09 ± 0.89	2.62 ± 0.28	–
OSL-E-22	SC39, 225-240	61 ± 6/44 ± 5	49 ± 3	700 ± 50	20 ± 10	3.56 ± 0.37/3.30 ± 0.35	0.16 ± 0.02	CG *(0.14)*	28.01 ± 2.43	7.87 ± 0.82/8.50 ± 0.89 *(7.05–9.39)*[a]	–
OSL-E-7	SC40, 53-63	51 ± 6/39 ± 4	57 ± 3	760 ± 80	10 ± 10	4.09 ± 0.20/3.88 ± 0.52	0.20 ± 0.02	CG *(0.14)*	5.05 ± 0.57	1.24 ± 0.16/1.30 ± 0.17 *(1.08–1.47)*[b]	IB
OSL-E-8	SC40, 91-101	62 ± 6/45 ± 5	59 ± 4	710 ± 70	20 ± 10	3.77 ± 0.24/3.51 ± 0.26	0.19 ± 0.02	CG *(0.14)*	9.85 ± 0.68	2.61 ± 0.24/2.81 ± 0.26 *(2.37–3.07)*[b]	–
OSL-E11	SC40, 129-139	55 ± 5/42 ± 5	57 ± 3	750 ± 80	15 ± 10	3.88 ± 0.36/3.67 ± 0.43	0.16 ± 0.02	CG *(0.14)*	12.07 ± 1.14	3.11 ± 0.36/3.29 ± 0.39 *(2.75–3.68)*[b]	IB
OSL-E10	SC40, 192-202	59 ± 5/48 ± 5	53 ± 3	730 ± 70	20 ± 10	3.67 ± 0.35/3.50 ± 0.34	0.16 ± 0.02	CG *(0.14)*	21.52 ± 1.60	5.87 ± 0.57/6.16 ± 0.60 *(5.30–6.76)*[a]	–
OSL-E-9	SC40, 229-239	68 ± 7/47 ± 5	60 ± 4	750 ± 80	20 ± 10	3.70 ± 0.30/3.64 ± 0.28	0.18 ± 0.02	CG *(0.14)*	45.05 ± 1.74	11.35 ± 0.85/12.36 ± 0.95 *(10.50–13.31)*[a]	–
OSL-E-3	SC58, 35-45	50 ± 5	54 ± 3	710 ± 70	20 ± 10	3.53 ± 0.50	0.21 ± 0.02	CG *(0.14)*	1.51 ± 0.19	0.43 ± 0.06	IB
OSL-E-4	SC58, 75-85	69 ± 6/47 ± 5	60 ± 4	740 ± 80	20 ± 10	3.97 ± 0.25/3.63 ± 0.24	0.19 ± 0.02	CG *(0.14)*	~3.2[5]	0.88–0.81[5,a,b]	–
OSL-E-5	SC58, 145-155	62 ± 6/46 ± 5	59 ± 3	760 ± 80	20 ± 10	3.88 ± 0.35/3.64 ± 0.33	0.17 ± 0.02	CG *(0.14)*	27.41 ± 1.72	7.06 ± 0.63/7.54 ± 0.69 *(6.43–8.23)*[b]	–
OSL-E-6	SC58, 184-194	78 ± 7/47 ± 5	58 ± 4	740 ± 80	20 ± 10	4.07 ± 0.32/3.58 ± 0.30	0.16 ± 0.02	CG *(0.14)*	41.03 ± 2.01	10.08 ± 0.79/11.47 ± 0.95 *(9.29–12.42)*[a]	–
OSL-E16	SC72, 70-85	50 ± 3/45 ± 5	37 ± 4	770 ± 80	20 ± 10	3.43 ± 0.43/3.36 ± 0.43	0.19 ± 0.02	CG *(0.14)*	1.04 ± 0.11	0.30 ± 0.04/0.31 ± 0.04 *(0.26–0.35)*[b]	–
Trebnitz											
OSL-E-17	TC9, 36-47	44 ± 3/36 ± 4	49 ± 3	800 ± 80	20 ± 10	3.59 ± 0.02/3.49 ± 0.44	0.21 ± 0.02	CG *(0.16)*	0.66 ± 0.07	0.18 ± 0.02/0.19 ± 0.02 *(0.16–0.21)*[b]	–
OSL-E-18	TC9, 85-95	41 ± 5	50 ± 3	780 ± 80	20 ± 10	3.50 ± 0.14	0.19 ± 0.02	CG *(0.16)*	3.39 ± 0.42	0.97 ± 0.14	-[7]
OSL-E-19	TC9, 168-183	43 ± 5	45 ± 3	720 ± 50	10 ± 10	3.62 ± 0.41	0.17 ± 0.02	CG *(0.16)*	16.26 ± 1.49	4.49 ± 0.50	–
OSL-E-20	TC9, 220-235	51 ± 3/40 ± 5	52 ± 3	790 ± 80	20 ± 10	3.67 ± 0.37/3.50 ± 0.37	0.16 ± 0.02	CG *(0.16)*	22.78 ± 1.78	6.20 ± 0.63/6.50 ± 0.68 *(5.57–7.18)*[a,b]	IB
OSL-E-21	TC9, 336-346	63 ± 4/43 ± 5	60 ± 4	880 ± 50	20 ± 10	7.85 ± 0.53/	0.14 ± 0.01	FG	97.24 ± 2.93	12.38 ± 0.83/13.85 ± 0.91 *(11.55–14.76)*[a,b]	IB

(*continued on next page*)

Table 2 (*continued*)

Lab number	Core and sample depth [cm]	U max./min.[1] [Bq/kg]	Th [Bq/kg]	K [Bq/kg]	Assumed water content [%]	Total dose rate max./min.[1] [Gy/ka]	Cosmic dose rate [Gy/ka]	Measurement technique[2] *(Sigma b[3])*	Equivalent dose [Gy]	Age min./max[1] *(resulting max. age range[4])* [ka]	Possible cause of over-/underestimation[6]
						7.02 ± 0.46					
OSL-E-33	TC12, 217-227	59 ± 4/34 ± 5	58 ± 4	870 ± 50	20 ± 10	7.60 ± 0.64/6.56 ± 0.54	0.16 ± 0.02	FG	103.7 ± 6.19	13.64 ± 1.15/15.80 ± 1.30 *(12.49–17.1)*[a,b]	IB
OSL-E-34	TC21, 210-230	56 ± 4/47 ± 4	53 ± 2	830 ± 60	20 ± 10	3.87 ± 0.51/3.73 ± 0.50	0.16 ± 0.02	CG *(0.16)*	1.92 ± 0.23	0.50 ± 0.07/0.51 ± 0.07 *(0.43–0.58)*[a]	–
OSL-E-29	TC22, 125-135	50 ± 6	53 ± 3	770 ± 80	10 ± 10	4.00 ± 0.51	0.16 ± 0.02	CG *(0.16)*	2.07 ± 0.22	0.52 ± 0.07	–
OSL-E-30	TC22, 180-190	46 ± 3/35 ± 5	54 ± 4	890 ± 60	20 ± 10	3.89 ± 0.81/3.72 ± 0.23	0.17 ± 0.02	CG *(0.16)*	4.15 ± 0.83	1.07 ± 0.22/1.12 ± 0.23 *(0.85–1.35)*[b]	IB
OSL-E-35	TC30, 50-60	42 ± 3/31 ± 3	45 ± 2	860 ± 60	10 ± 10	4.03 ± 0.62/3.84 ± 0.59	0.20 ± 0.02	CG *(0.16)*	2.02 ± 0.28	0.50 ± 0.08/0.52 ± 0.08 *(0.42–0.60)*[b]	–
OSL-E-13	TC32, 30-40	86 ± 5/51 ± 5	51 ± 3	750 ± 80	10 ± 10	4.55 ± 0.70/3.96 ± 0.62	0.21 ± 0.02	CG *(0.16)*	0.36 ± 0.05	0.08 ± 0.01/0.09 ± 0.01 *(0.07–0.10)*[a,b]	H
OSL-E-14	TC32, 80-90	48 ± 3/39 ± 4	52 ± 3	820 ± 80	20 ± 10	3.73 ± 0.39/3.59 ± 0.38	0.19 ± 0.02	CG *(0.16)*	1.49 ± 0.12	0.40 ± 0.04/0.42 ± 0.04 *(0.36–0.46)*[b]	–
OSL-E-15	TC32, 170-180	47 ± 3/39 ± 5	52 ± 3	920 ± 60	20 ± 10	3.96 ± 0.49/3.83 ± 0.48	0.17 ± 0.02	CG *(0.16)*	2.55 ± 0.28	0.65 ± 0.08/0.67 ± 0.08 *(0.57–0.75)*[b]	–
Meilitz											
OSL-E-31	MC2, 40-50	51 ± 3/42 ± 5	62 ± 4	680 ± 40	15 ± 10	3.75 ± 0.05/3.61 ± 0.05	0.21 ± 0.02	CG *(0.21)*	1.17 ± 0.17	0.31 ± 0.05/0.32 ± 0.05 *(0.26–0.37)*[b]	–
OSL-E-32	MC2, 80-90	53 ± 6	65 ± 4	650 ± 40	10 ± 10	3.94 ± 0.46	0.19 ± 0.02	CG *(0.21)*	1.79 ± 0.18	0.46 ± 0.05	–
OSL-E-36	MC15, 40-55	63 ± 7/43 ± 4	59 ± 3	650 ± 50	10 ± 10	4.02 ± 0.61/3.67 ± 0.56	0.20 ± 0.02	CG *(0.21)*	1.01 ± 0.14	0.25 ± 0.04/0.28 ± 0.04 *(0.21–0.32)*[b]	–
OSL-E-23	MC35, 75-90	59 ± 7/37 ± 5	56 ± 3	650 ± 70	10 ± 10	3.89 ± 0.26/3.52 ± 0.25	0.19 ± 0.02	CG *(0.21)*	~3.8[5]	0.98–1.08[5,b]	IB
OSL-E-37	MC43, 80-90	60 ± 5/42 ± 4	57 ± 3	660 ± 50	10 ± 10	3.95 ± 0.35/3.65 ± 0.33	0.19 ± 0.02	CG *(0.21)*	8.71 ± 0.59	2.20 ± 0.20/2.39 ± 0.22 *(2.00–2.61)*[b]	–
OSL-E-24	MC53, 57-72	70 ± 7/46 ± 5	62 ± 4	690 ± 40	20 ± 10	3.90 ± 0.43/3.53 ± 0.39	0.20 ± 0.02	CG *(0.21)*	6.06 ± 0.59	1.56 ± 0.17/1.72 ± 0.19 *(1.39–1.91)*[b]	–
OSL-E-25	MC53, 103-118	65 ± 6/41 ± 4	59 ± 4	670 ± 40	20 ± 10	3.71 ± 0.40/3.34 ± 0.34	0.19 ± 0.02	CG *(0.21)*	7.57 ± 0.64	2.04 ± 0.20/2.27 ± 0.29 *(1.84–2.56)*[b]	–
OSL-E-26	MC71, 39-54	68 ± 7/46 ± 5	63 ± 4	820 ± 50	20 ± 10	4.22 ± 0.44/3.88 ± 0.41	0.21 ± 0.02	CG *(0.21)*	9.89 ± 0.89	2.35 ± 0.25/2.55 ± 0.27 *(2.10–2.82)*[b]	–
OSL-E-27	MC71, 94-109	74 ± 7/48 ± 5	64 ± 4	770 ± 50	20 ± 10	4.18 ± 0.51/3.78 ± 0.47	0.19 ± 0.02	CG *(0.21)*	27.73 ± 3.05	6.64 ± 0.81/7.34 ± 0.91 *(5.83–8.25)*[b]	–
OSL-E-28	MC71, 151-166	55 ± 6/42 ± 5	60 ± 4	710 ± 70	15 ± 10	3.84 ± 0.40/3.63 ± 0.38	0.17 ± 0.02	CG *(0.21)*	46.00 ± 3.80	11.98 ± 1.25/12.68 ± 1.34 *(10.73–14.02)*[b]	IB

[1] In case of radioactive disequilibrium in the ^{238}U decay chain (a = disequilibrium between ^{238}U and ^{226}Ra; b = disequilibrium between ^{226}Ra and ^{210}Pb; information given in the age row).
[2] CG = coarse grain (quartz OSL), FG = fine grain (polymineral pIR-IRSL).
[3] Used for age calculation when using the minimum age model (Galbraith et al., 1999).
[4] The maximal age range gives the range within which the true sedimentation age should be situated, and was for simplification used in this paper. It was determined by subtracting its error from the minimum age and adding its error to the maximum age.
[5] De taken from lower outlier population. In this case no error was given, but just the age range resulting from the radioactive disequilibrium.
[6] IB = incomplete bleaching, H = human activity such as (occasional) deep ploughing.
[7] possibly linked with pedogenesis of T-PS-1.

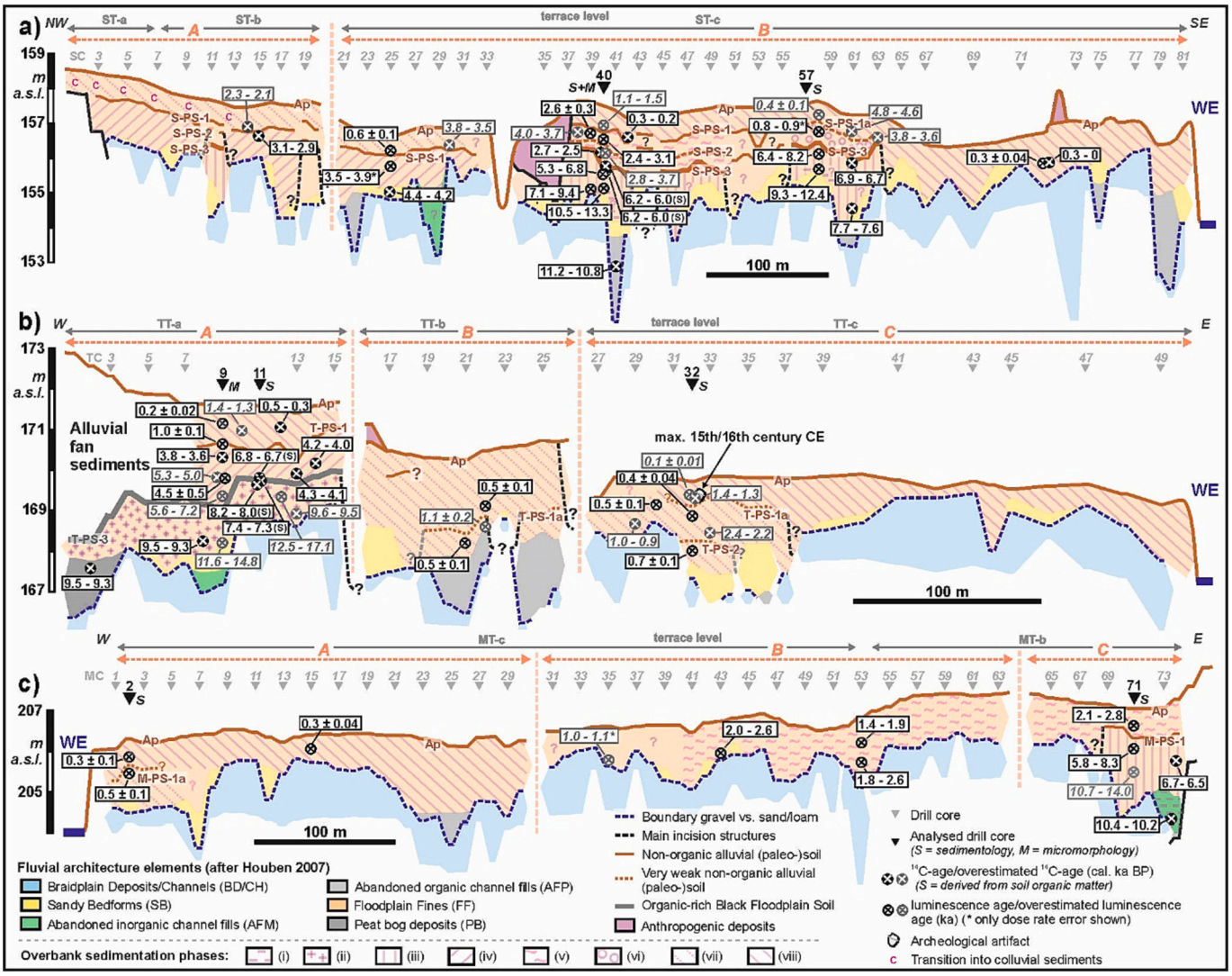

Fig. 3. The studied transects with radiocarbon and luminescence ages, sediments belonging to different overbank sedimentation phases (defined based on stratigraphical features and numerical dating; see Figs. 7 and 8), and the positions of analyzed cores: (a) Salsitz. The radiocarbon ages of this transect were taken from Ballasus et al. (2022a), but re-calibrated using the Intcal20 calibration curve (Reimer et al., 2020). (b) Trebnitz, (c) Meilitz.
The locations of the transects, including the spatial distributions of the terrace levels, are given in Fig. 2.
WE = Weiße Elster River, Ap = plough horizon.

- **Archaeological dating:** Each site was registered on four different chronological levels with increasing resolution: epoch, period, phase and sub-phase (Eggert, 2012, Eggert and Samida, 2013), and classified according to the chronological system for the prehistory and early history in Central Germany.
- **Site function:** Based on the available information in the archaeological publications and local area files, we distinguished three site types: (i) Settlements indicated by pits, post-holes, grinding stones, loom weights, spindle whorls and/or pottery fragments, and (ii) Burial sites indicated by human remains. Therefore, a site was registered twice whenever a burial was documented within a settlement. (iii) Stray finds, including single objects or assemblages with little or no context information, i.e. either lost objects or material remains from settlements or burial sites that have not yet been identified as such (Schülke, 2011; Hinz, 2014).
- **Geographic location:** We distinguished between sites with a precise location, and sites that cannot be located due to missing or poor geographic information. The latter were associated with symbolic/fuzzy coordinates, i.e., either with their presumed location or the

church of the village in whose district the site was discovered (cf. Ostritz, 2000).

Finally, we combined precisely located sites that (i) were <250 m apart from each other, (ii) associated with the same or compatible dating (e.g., "Bronze Age" + "Bronze Age", Early Bronze Age + "Bronze Age", etc.), and (iii) interpreted in the same or compatible manner (e.g. settlement + settlement, settlement + stray finds, etc.). This combination allows systematic statements with respect to site distribution patterns, and reduces the risk of overrating geographical parameters in spatial analyses (cf. Hilbig, 1993; Mischka, 2007; Pankau, 2007).

3.3.1.1.

To investigate diachronic changes in settlement intensity, we used the parameter *site frequency per century* (German: Fundstellenfrequenz) which was already previously used by Ahlrichs et al. (2018) and Miera et al. (2019, 2022) to compare varying settlement intensities on a (supra-)regional scale. The parameter was calculated for each period individually, as their duration varies (Schmotz, 1989; Paetzold, 1992):

$$\text{Frequency per century} = Sn/Pn*100$$

(Sn = number of sites, Pn = duration of respective period in years).

However, we did not consider all sites equally, but applied different factors according to the site category (settlements: 1, burial sites: 0.5, stray finds: 0.25). This is based on the assumption that human impact on the environment is most pronounced in the immediate vicinity of settlements, whereas a comparatively reduced human impact can be expected in the immediate vicinity of burial sites. Unless proven otherwise, stray finds indicate only a brief human presence with a likely minimal environmental impact (also see supporting text TE-1).

3.3.2. Recording and pre-processing of written historical data

To gain insights into Medieval and Early Modern settlement activity beyond archaeological data analysis covering the period up to 1200 CE (Section 3.3.1), we built up a historical database (Fütterer, 2016). First, all recent settlements of the study area were compiled from freely available OpenStreetMap data. These data were thoroughly reviewed using current topographical and historical maps (e.g., the Sächsische Meilenblätter or Historische Messtischblätter), since according to different administrative divisions of the individual federal states, either several settlements are combined into one municipality, or villages merged into cities and deserted villages are not recorded separately. Subsequently, to discriminate different settlement phases, the year of its first mentioning was determined for each settlement using various overview literature (Eichler et al., 1983, 1985; Eichler and Walther, 1984, 2001; Rosenkranz, 1982; Kahl, 2010; Autorenkollektiv, 1976, 1986; Joseph and Porada, 2006) and the Historisches Ortsverzeichnis Sachsen (Historical Gazetteer Saxony; https://hov.isgv.de/) (also see supporting text TE-2a). To minimize the difference between settlement foundation and its first written documentation as far as possible, this information was complemented by information from the archaeological database (Section 3.3.1). For this purpose, archaeological sites with an assured Medieval classification were extracted, allowing for 195 settlements a more exact chronological classification into Early, High or Late Middle Ages. Subsequently, information on the archaeological dating of the settlements was partly supplemented from the literature (e.g. Timpel and Spazier, 2014; Kenzler, 2012).

To determine the settlement intensity for selected periods, the "first evidence" was determined either from the first written mention or archaeological dating. The first written mention was taken if no archaeological finds allowed a different dating. In case of an archaeological classification into Early, High and Late Middle Ages, the first evidence was the end point of the period (Early Middle Ages: 900 CE, High Middle Ages: 1250 CE, Late Middle Ages: 1500 CE). If the first written mention was before the end of the archaeological period, this date was taken as the first evidence (also see supporting text TE-2b).

4. Results

4.1. Chronology

The radiocarbon ages can be found in Table 1, and the analytical results of luminescence measurements are given in Table 2. The combined radiocarbon and luminescence ages encompass the Latest Pleistocene and Holocene: For Salsitz they vary between 13.3 - 10.5 ka and 0.3–0 cal. ka BP, for Trebnitz between 17.1 - 12.5 ka and 0.1 ± 0.01 ka, and for Meilitz between 14.0 - 10.7 ka and 0.3 ± 1 ka (Fig. 3, Tables 1 and 2). Given strong groundwater influence in the floodplain causing partly significant radioactive disequilibria, several luminescence ages can only be given as minimal and maximal ages with total differences of up to >2 ka, and to simplify their presentation we give them as age ranges that were determined by subtracting its error from the minimum age and adding its error to the maximum age (Table 2). Furthermore, for three luminescence samples (OSL-E-2, 4, 23), the equivalent dose (De) distributions showed significant lower outlier populations that were used for age calculation (for the equivalent dose distributions see Supporting Figs. S-1 to S-3). Since there were too few aliquots forming these lower outlier peaks, no error was calculated for these De's. Hence, only the age range resulting from the dose rate errors is given.

4.2. Sediment properties

The analytical values of the six representative cores are shown in Fig. 4 (values see in supporting tables TA-1–TA-6). The recent anthropogenic Ap-horizons significantly differ from the lower parts of the cores by often strongly increased values of mass-specific susceptibility, TOC and P_{total}. By contrast, most paleosols, only weakly recognizable in the field by e.g. more intensive iron/manganese stains and concretions and/or different grain sizes, colors or structures compared with over- and underlying material, are also hardly directly recognizable by their analytical values. Instead, they can often only indirectly be identified by different properties of their overlying sediments such as different (often more sandy) grain sizes and values of TOC, mass-specific magnetic susceptibility or the Rb/Sr-ratio. An exception is paleosol T-PS-3 ("Black Floodplain Soil") in core TC11, showing significantly increased TOC-values compared with the over- and underlying sediments of up to 1.15 %. Below the Ap-horizons, upwards increasing P_{total} values in paleosol S-PS-3 in core SC40 and strongly enhanced values of mass-specific susceptibility and TOC in the uppermost sediments of core TC32 suggest direct anthropogenic impact in the floodplain such as agriculture or settlement activities (Crowther, 2003; Holliday and Gartner, 2007). Apart from some Ap-horizons and their directly underlying sediments, the uppermost sediments in core TC32 and the sediments overlying paleosol T-PS-1 in core TC11 with carbonate contents up to 15 %, the sediments are largely carbonate-free. In most cores but core MC71, the elemental ratio Rb/Sr systematically decreases upwards.

Micromorphological analysis of core SC40 showed slightly advanced development of paleosols S-PS1 and 2 compared to the parent material, indicated by more developed pedogenic aggregation, clay coatings (usually disturbed, partly dusty) and depletion features (Table 3; Fig. 5a–c). Paleosol S-PS-3 (sample 7) shows well expressed clay coatings, Fe-nodules and depletion hypercoatings, which demonstrates advanced pedogenesis (stagnic Luvisol subsoil; IUSS Working Group WRB, 2022). Furthermore, especially in the upper part of the sequence Fe-/Mn-nodules linked with varying hydrological conditions are ubiquitously found (Fig. 5a), and some fine charcoal was detected in paleosol S-PS-3.

Micromorphological analysis of core TC9 showed an intensive subangular blocky structure, clay coatings, numerous Fe-/Mn-nodules and fine charcoal for paleosol T-PS-3 ("Black Floodplain Soil" corresponding to a humic Gleysol, IUSS Working Group WRB, 2022), demonstrating

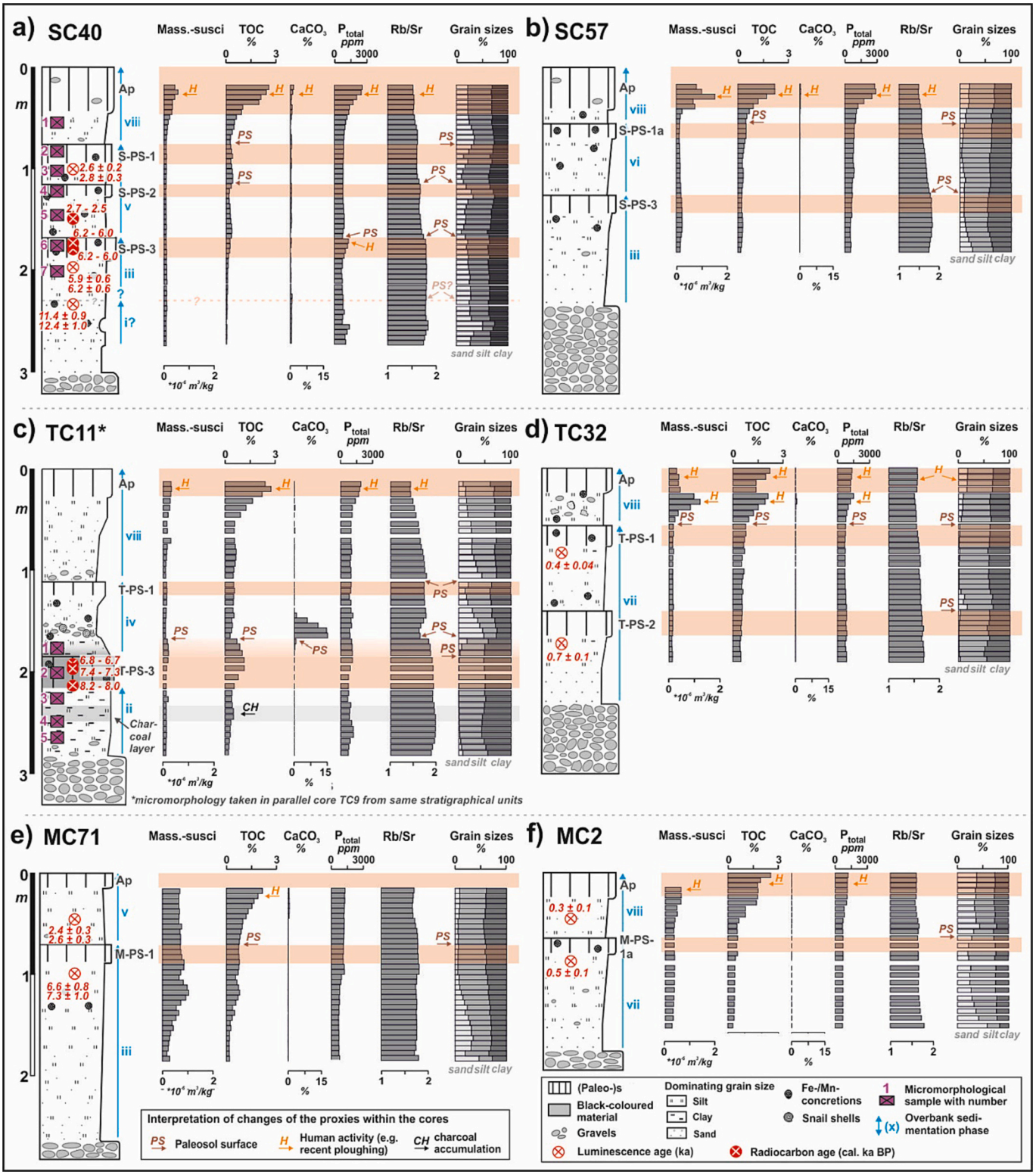

Fig. 4. Profile drawings of the six analyzed cores with overbank sedimentation phases and analytical values with interpretations from Salsitz (a, b), Trebnitz (c, d), and Meilitz (e, f). Furthermore, numerical ages from these cores probably representing sedimentation ages are shown.

intensive pedogenesis under varying hydrological conditions and some influence of fire (Table 3; Fig. 5d, f). The "Black Floodplain Soil" formed close to the groundwater table, and was later buried by sediment and overprinted by illuvial clay from above terrestrial pedogenesis. The underlying deposits are entirely apedal, without clay coatings, exhibiting various amounts of Fe-/Mn-nodules. Furthermore, a darker-colored layer within these deposits showed finely layered charcoal fragments (Fig. 5f), explaining its increased TOC-content and darker color.

4.3. Former settlement patterns

In total, 991 sites were entered into in the archaeological database.

Table 3
Selected parameters and interpretations of the micromorphological analyses of cores SC40 (Salsitz) and TC9 (Trebnitz) (sample locations please see Fig. 4a, c). Red colors indicate intensive, and yellow colors less intensive features.

core	sample number	microstructure: aggregation				groundmass: b-fabric				pedofeatures											charcoal	interpretation
											limpid clay coatings			dusty clay coatings			Fe(-Mn) nodules					
		granular	subangular blocky	angular blocky	apedal	speckled	striated	porostriated	granostriated	depletion	fragments	disturbed	in situ	fragments	disturbed	in situ	typic/nucleic	concentric	aggregatic	denthritic		
SC40	1																					Overbank deposit
	2 *(S-PS-1)*																					Weak soil
	3																					Overbank deposit
	4 *(S-PS-2)*																					Soil
	5																					Overbank deposit
	6 *(S-PS-3)*																					Intensive soil (Stagnic Luvisol)
	7																					Subsoil
TC9	1																					Transition to sediment with pedogenic overprinting
	2 *(T-PS-3)*																					Humic gleysoil
	3																					Overbank deposit
	4																					Overbank deposit, upper part layered charcoal
	5																					Overbank deposit

The results for the different archaeological periods and epochs are shown in Table 4, and were discriminated for each site according to the total site sub-catchment and a smaller local site sub-catchment up to 10 km upstream (see Fig. 6a for their locations). Furthermore, a map of the exemplary Urnfield Period is shown in Fig. 6b. Settlement activity in the total and local site sub-catchments of downstream sites Salsitz and Trebnitz clearly started since the Early Neolithic, whereas around upstream site Meilitz significant settlement activity clearly only started since the Late Neolithic and especially since the Late Bronze Age. However, several (Early) Neolithic stray finds in the sub-catchments of the latter site potentially indicate an earlier start of intensive human occupation also here (Table 4). Generally, the settlement intensities strongly varied between the individual periods, with significant gaps during the Middle Neolithic, Early Bronze Age and Migration Period. The highest absolute values are recorded for the High Middle Ages, but an increasing trend can already be observed since the Early Middle Ages. Despite different absolute values, except for the time between the Late Bronze Age and Roman Period the relative trends of settlement intensity are similar for the total and local site sub-catchments.

Furthermore, 738 village foundations were recorded in the historical database between 800 and 1600 CE (for the earlier period also complemented by archaeological information). These data show that most settlements were founded between 1200 and 1400 CE, what also included the upstream catchment of the Weiße Elster River (Table 5, Fig. 6c).

5. Discussion

5.1. Chronostratigraphies of the studied sites

By combining our new radiocarbon and luminescence ages, sedimentological and micromorphological analyses with the previously published transect stratigraphies (von Suchodoletz et al., 2022) and radiocarbon ages for Salsitz (Ballasus et al., 2022a), we could build up well-resolved chronostratigraphies for the studied transects (Figs. 3, 7). This comprehensive chronostratigraphic context also allowed to identify over-and underestimated ages, i.e., radiocarbon ages obtained from older organic material that was incorporated into younger sediments (Lang and Hönscheidt, 1999), and luminescence ages of material that was not completely bleached during fluvial transport or was influenced by human activity such as recent deep ploughing (Jain et al., 2004, von Suchodoletz et al., 2023) (over−/underestimated ages marked in grey and italic in Fig. 3; possible causes see in Table 2). Hence, in the following, we only use ages that probably represent real sedimentation ages:

* Salsitz (Fig. 3a): The oldest overbank deposits in the central part of terrace level ST-c, yielding ages of 13.3–10.5 ka (core SC40) and 12.4–9.3 ka (core SC58), overlie an abandoned organic channel fill that was dated to 11.2–10.8 cal. ka BP (core SC41). This layer is obviously only few decimeters thick and must be incomplete, what is suggested by Middle Holocene ages of 9.4–7.1 ka (core SC39) and 7.7–7.6 cal. ka BP (core SC61) from similar stratigraphical positions in neighboring cores, i.e. also taken near the base of the overbank deposits. Unfortunately, the millennia-long hiatus between both layers could not be recognized in the field, and – if at all – only by a very small change of the grain sizes in the analytical data (Fig. 4a). The next sediment generation of Middle Holocene age was dated between 9.4 - 7.1 ka (core SC39) and 6.8–5.3 ka (core SC 40). Accordingly, two radiocarbon ages of bulk organic matter from well-developed paleosol S-PS-3 developed in the upper part of these sediments (see micromorphological Table 3) gave ages of 6.2–6.0 cal. ka BP (core SC40). Upwards increasing P_{total}-values in core SC40 indicate local human activity in the floodplain (Fig. 4a). The next sediment generation directly overlies fluvial gravels in terrace levels ST-a, ST-b and the western part of ST-c, and was dated between 4.4

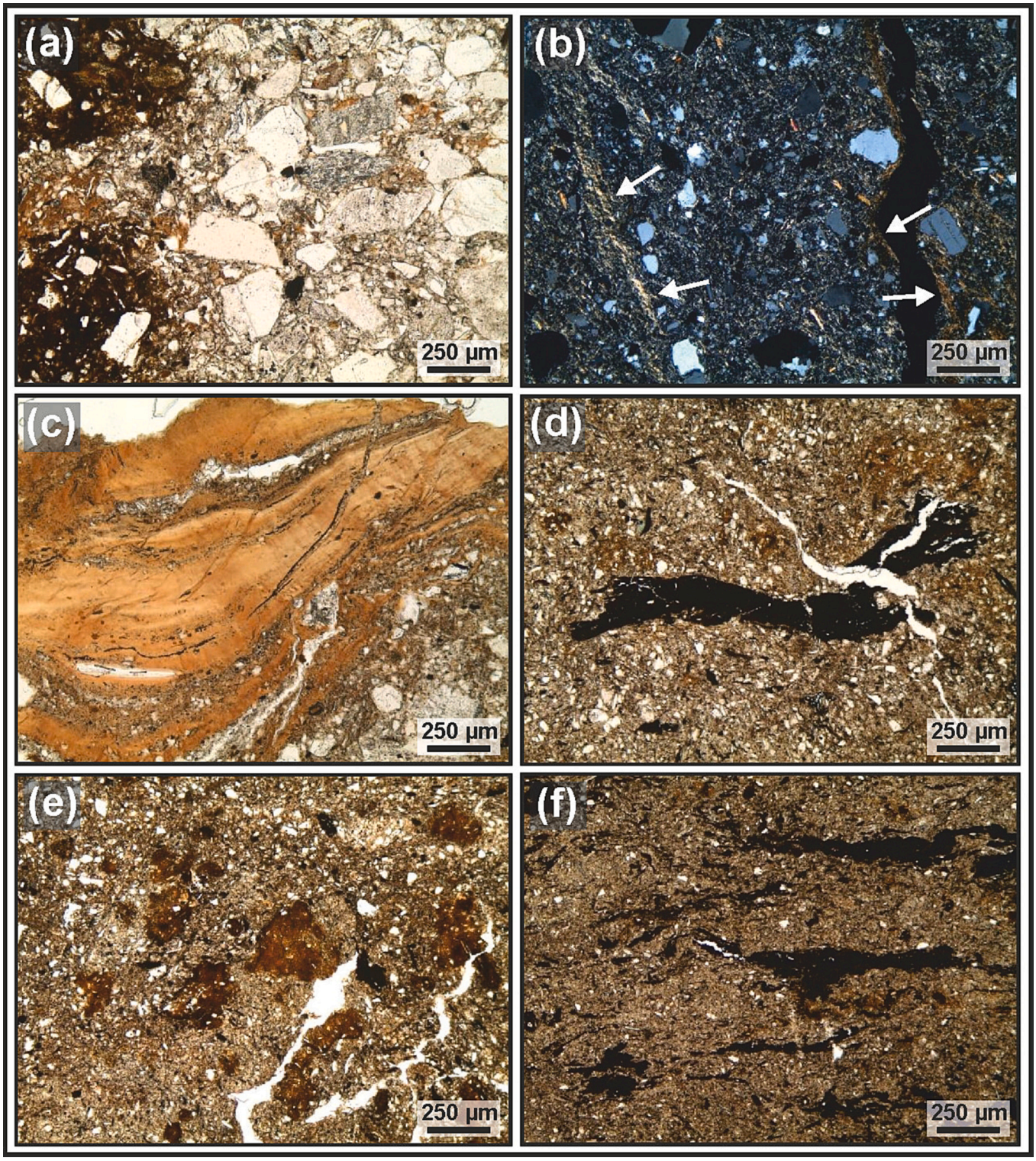

Fig. 5. Photos of selected micromorphological samples of: Core SC40 in transect Salsitz: (a) Sample 4 (paleosol S-PS-2): clay coatings associated with manganese nodules (left side) next to a pale, sand rich domain characterized by iron and clay depletion (PPL), (b) Sample 6 (paleosol S-PS-3): different types of clay within groundmass and along pores (white arrows; XPL), (c) Sample 7 (overbank sediment below S-PS-3): thick limpid and partly dusty clay coating related to clay illuviation (PPL).
Core TC9 in transect Trebnitz: (d) Sample 2 ("Black Floodplain Soil" T-PS-3): charred fragile material, (e) Sample 2 ("Black Floodplain" Soil T-PS-3): iron nodules (PPL), (f) Sample 3 (overbank sediment): layered charcoal fragments.

Table 4
Settlement activity in the study area since the Early Neolithic based on archaeological data.

Period	Duration (years)	Meilitz			Trebnitz			Salsitz		
		Settlements	Burial sites	Stray finds	Settlements	Burial sites	Stray finds	Settlements	Burial sites	Stray finds
(a) Total site sub-catchments										
Early Neolithic	1100	0	0	8	40	0	24	61	0	45
Middle Neolithic	1600	0	0	0	1	1	0	2	1	0
Late Neolithic	500	0	2	9	10	19	32	11	20	38
Neolithic - unclassified[a]	*3200*	*0*	*0*	*66*	*21*	*11*	*278*	*31*	*11*	*326*
Early Bronze Age	700	1	0	1	2	0	4	2	0	4
Middle Bronze Age	300	1	0	1	1	0	2	1	0	2
Late Bronze Age	100	3	3	0	3	5	0	3	5	0
Urnfield Culture	400	15	4	5	24	13	8	24	14	8
Bronze Age – unclassified[a]	*1500*	*2*	*1*	*1*	*11*	*4*	*10*	*14*	*4*	*12*
Hallstatt period	350	14	3	2	16	3	4	16	3	4
La Tène period	450	3	5	2	9	10	5	10	11	5
Pre-Roman Iron Ages - unclassified[a]	*800*	*0*	*0*	*0*	*2*	*0*	*0*	*4*	*0*	*1*
Roman Empire	375	2	0	2	6	1	8	7	2	10
Migration Period	195	0	0	0	0	1	1	0	1	1
Early Middle Ages	330	4	2	3	16	16	32	17	18	33
High Middle Ages	350	29	3	4	52	7	20	53	7	25
Middle Ages - unclassified[a]	*680*	*31*	*2*	*13*	*49*	*14*	*38*	*53*	*15*	*42*
(b) Local site sub-catchments up to 10 km upstream										
Early Neolithic	1100	0	0	1	7	0	10	22	0	22
Middle Neolithic	1600	0	0	0	0	1	0	1	0	0
Late Neolithic	500	0	2	6	5	7	14	1	1	9
Neolithic - unclassified[a]	*3200*	*0*	*0*	*34*	*9*	*5*	*93*	*11*	*1*	*56*
Early Bronze Age	700	1	0	0	0	0	3	0	0	0
Middle Bronze Age	300	0	0	0	0	0	0	0	0	0
Late Bronze Age	100	1	2	0	0	1	0	0	0	0
Urnfield Culture	400	2	1	1	1	3	1	0	1	0
Bronze Age - unclassified[a]	*1500*	*0*	*0*	*1*	*2*	*1*	*4*	*3*	*0*	*2*
Hallstatt period	350	1	0	1	0	0	1	0	0	0
La Tène period	450	1	2	1	1	1	1	2	1	0
Pre-Roman Iron Age - unclassified[a]	*800*	*0*	*0*	*0*	*1*	*0*	*0*	*2*	*0*	*1*
Roman Empire	375	1	0	0	0	0	3	1	1	2
Migration Period	195	0	0	0	0	0	0	0	0	0
Early Middle Ages	330	3	2	3	1	4	7	2	2	1
High Middle Ages	350	8	1	3	6	0	4	2	0	5
Middle Ages - unclassified[a]	*680*	*12*	*1*	*12*	*7*	*2*	*8*	*6*	*1*	*4*

[a] These lines indicate finds that could chronologically not further be classified.

and 4.2 cal. ka BP (core SC25) and 3.1–2.9 cal. ka BP (core SC15). In the central part of terrace level ST-c (between cores SC38 and SC42), sediments overlying paleosol S-PS-3 show lower clay contents and Rb/Sr-ratios compared with the underlying sediments. This indicates a higher energetic fluvial environment and less pre-weathered material compared with the Middle Holocene (Fig. 4a). These sediments were dated to 2.7–2.5 cal. ka BP and 2.6 ± 0.3 ka (both core SC40), and contain an intercalated weak paleosol (S-PS-2) (see Table 3). The upper package shows lower Rb/Sr-ratios compared with the lower, indicating another change towards less pre-weathered material (Fig. 4a). The following sediment generation, found between paleosols S-PS-3 and S-PS-1a in the central part of terrace level ST-c (between cores SC56 and SC63), was dated to ca. 0.8–0.9 ka (core SC58), and also showed lower Rb/Sr-rations and clay contents compared with the underlying Middle Holocene sediments (Fig. 4b). Finally, the youngest sediments overlie paleosol S-PS-1 in terrace levels ST-a, ST-b and the western and central part of ST-c, passing over into colluvial slope sediments northwestwards, and directly overlie gravels in the eastern part of ST-c. These sediments show higher sand contents and mass-specific magnetic susceptibility values compared with the underlying material (Fig. 4a, b), indicating a high-energetic fluvial environment and stronger input of magnetically susceptible material. They were dated between 0.6 ± 0.1 ka (core SC25) in the western and 0.3–0 cal. ka BP (core SC72) in the eastern part of terrace level ST-c.

* Trebnitz (Fig. 3b): The oldest overbank sediments with clay contents up to 57 % (Fig. 4c), partly overlying a basal peat that was dated to 9.5–9.3 cal. ka BP (core TC2), are found in terrace level TT-a. Embedded charcoal also gave an age of 9.5–9.3 cal. ka BP (core TC8), i.e., their deposition obviously relatively abruptly interrupted peat growth. A concentration of layered charcoal in these sediments (Table 3; Fig. 5f) indicates strong fire activity around the site during its deposition. Bulk organic matter of the overprinting organic- and clay-rich “Black Floodplain Soil” (paleosol T-PS-3), showing TOC contents up to 1.15 % and clay contents up to 52 % (Fig. 4c), was dated between 8.2 - 8.0 and 6.8–6.7 cal. ka BP (core TC9). This demonstrates very low intense Middle Holocene fine-grained background sedimentation in a wet floodplain environment with synsedimentary pedogenesis. Systematically upwards-coarsening grain sizes and decreasing TOC-values in its uppermost part (Fig. 4c) indicate its gradual transition into very sandy fluvial sediments, and carbonate contents up to 15 % in the latter demonstrate the input of tufa-derived material from the western tributary Buchenheimer Bach (Fig. 2b). This indicates high-energy fluvial sedimentation with strong lateral sediment input following "Black Floodplain Soil" formation. Accordingly, lower Rb/Sr-rations compared with the underlying sediments show a change towards less pre-weathered material (Fig. 4a). These sediments were dated between 4.3 - 4.1 cal. ka BP (core TC13, taken from the transition) and 3.8–3.6 cal. ka BP (both core TC9), and are overprinted by paleosol T-PS-1. Small

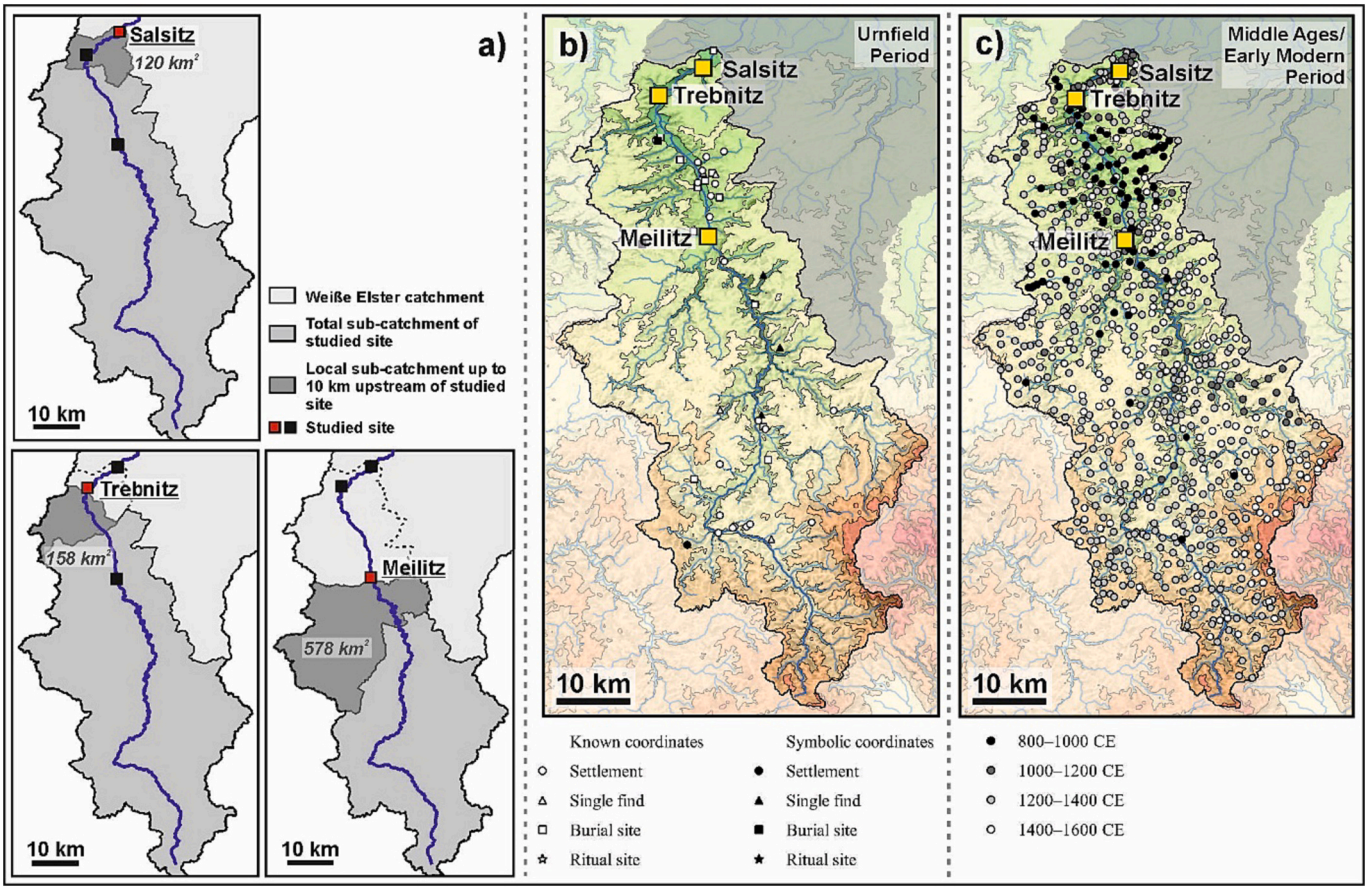

Fig. 6. Former settlement patterns in the study area: (a) Overview of the total and local (up to 10 km upstream from the site locations) site sub-catchments, (b) pattern of the Urnfield Period (3.2–2.8 ka) based on archaeological data, (c) pattern of the Middle Ages/Early Modern Period (village foundations) mainly based on written historical data.

Table 5
Number of foundations of villages in the study area between 800 and 1600 CE based on written historical data.

Period (CE)	Meilitz[a]	Trebnitz[a]	Salsitz[a]
800–1000	12/*9*	51/*11*	56/*20*
1000–1200	32/*5*	52/*9*	72/*32*
1200–1400	297/*109*	372/*24*	388/*39*
1400–1600	138/*37*	157/*6*	162/*12*

[a] Data for: Total site sub-catchment/*local site sub-catchment up to 10 km upstream*.

remains of the following sediment generation, overprinted by paleosol T-PS-2, are found in the western part of terrace level TT-c. These sediments were dated to 0.7 ± 0.1 ka (core TC32). The following sediment generation overlies paleosol T-PS-1 in terrace level TT-a, where its material possibly forms part of the alluvial fan sediments of the Buchenheimer Bach (Fig. 2b), and overlies paleosol T-PS-2 in the western part of TT-c. These sediments were dated between 0.5 ± 0.1 ka (cores TC21, TC22, TC30) and 0.2 ± 0.02 ka (core TC9). Coarser grain sizes compared with underlying material in cores TC11 and TC32 (Fig. 4c, d) indicate a higher-energy fluvial environment than before. In terrace level TT-b and the western part of TT-c these sediments are divided by weak paleosol T-PS-1a, obviously representing a rather short interruption of fluvial sedimentation. Potsherds and high values of mass-specific magnetic susceptibility, P_{total} and TOC of the sediments overlying paleosol T-PS-1a in core TC32 suggest human activity in the floodplain (Fig. 4d).

* Meilitz (Fig. 3c): The oldest fluvial sediments, abandoned inorganic channel fills, are found in the easternmost part of terrace level MT-b. These were dated to 10.4–10.2 cal. ka BP (core MC74). These sediments are overlain by overbank deposits that are only found in the eastern part of terrace level MT-b, and were overprinted by paleosol M-PS-1. These fining-up sediments show upwards increasing values of mass-specific susceptibility and TOC, the latter indicating strong direct input of eroded surficial slope material at least at this marginal floodplain position (Fig. 4e). They were dated to 8.3–5.8 ka (core MC71) and 6.7–6.6 cal. ka BP (core MC74). The next sediment generation was found in terrace level MT-b and the eastern part of MT-c overlying paleosol M-PS-1. These sediments were dated between 2.8 - 2.1 ka (core MC71) and 1.9–1.4 ka (core MC53), and high TOC-values in core MC71 indicate strong direct input of eroded surficial slope material (Fig. 4e). The next sediment generation was only found in the western part of terrace level MT-c, and was dated between 0.5 ± 0.1 and 0.3 ± 0.1 ka (both core MC2). These sediments are divided by weak paleosol M-PS-1a, representing a short interruption of fluvial sedimentation. Coarser grain sizes in the sediments overlying paleosol M-PS-1a indicate a higher-energy fluvial environment (Fig. 4f).

Our compilation confirms most of our former field-based stratigraphical and preliminary chronological classifications (von Suchodoletz et al., 2022). However, also some corrections were necessary, since our fluvial paleosols often showed only very slight optical differences with their over- and underlying sediment packages, making the direct visual comparison of several parallel cores necessary for their recognition. This resembles the situation in many other Central European

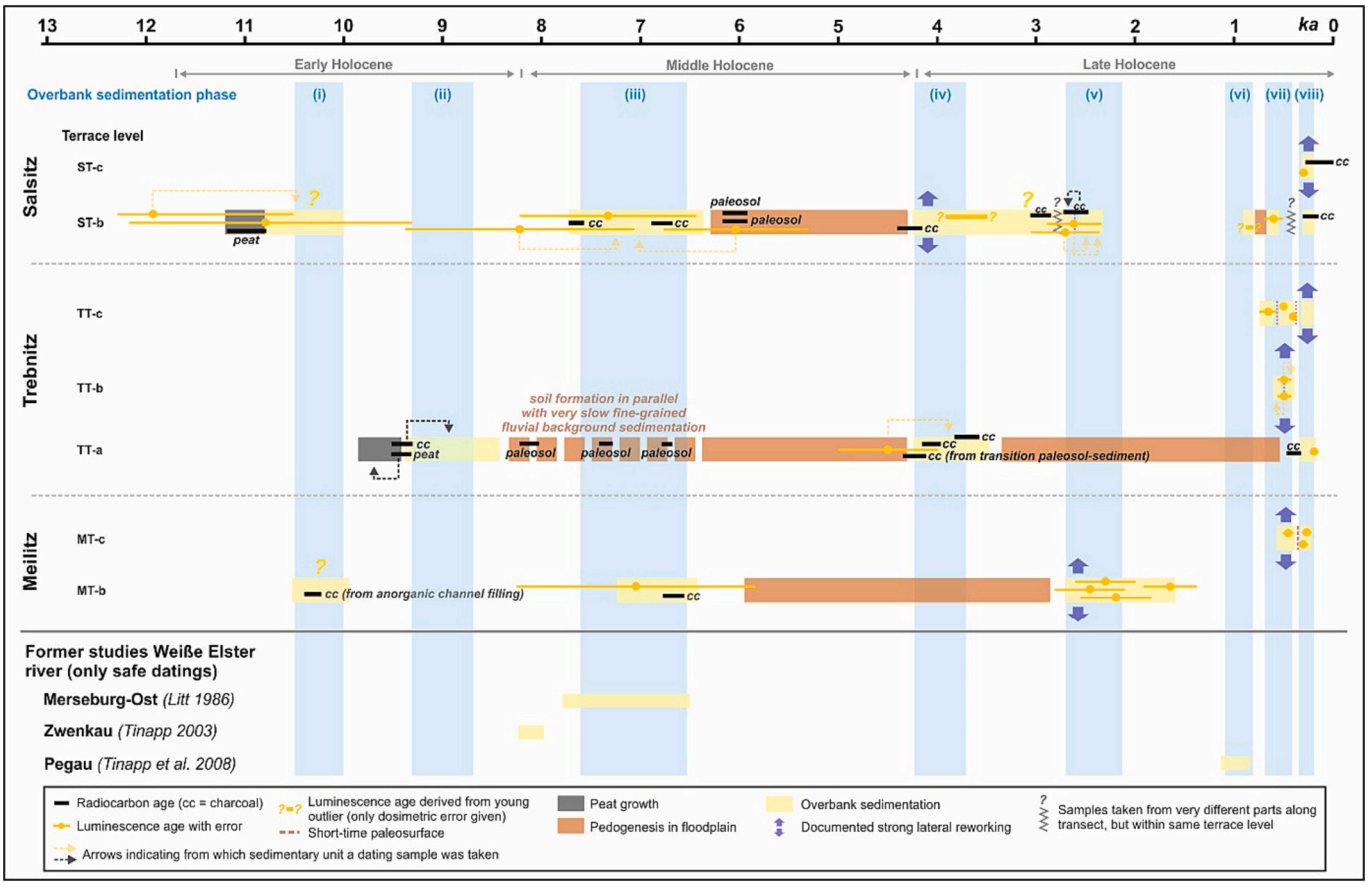

Fig. 7. Compilation of the overbank sedimentation phases at the studied transects in the middle Weiße Elster floodplain together with the numerical ages. Furthermore, phases of strong lateral reworking are shown. The subdivision of the Holocene relates to Walker et al. (2019).

floodplains where paleosols - indicating interruptions of fluvial sedimentation within the stratigraphies - were hardly stratigraphically detected (e.g., Notebaert et al., 2011; Fuchs et al., 2011). This contrasts with lower latitudes, where visibly well-developed Holocene fluvial paleosols can regularly be observed (e.g., Hall and Periman, 2007, May et al., 2015, von Suchodoletz and Faust, 2018).

- With respect to the stratigraphy, in Salsitz between cores SC56 and SC63 paleosol S-PS-3 had to be shifted to the position of former paleosol S-PS-2. Furthermore, also the obviously incomplete and thin layer of Early Holocene fine-grained sediments between cores SC38 and SC63 was not detected in the field. Otherwise, our field-based stratigraphy could be largely confirmed.
- With respect to the preliminary chronological classifications, in Salsitz the sediments between former paleosols S-PS-3 and S-PS-2 (between cores SC56 and SC63) were shifted from the (earlier) Late Holocene (fine-grained fluvial sediment generation [FFSG] II) to the Early to Middle Holocene. In Trebnitz, the lower sediments east of core TC15 were shifted from the (earlier) Late Holocene (FFSG II) to the last millennium. Finally, in Meilitz the lowest sediments between cores MC69 and MC74 were shifted from the (early) Late Holocene (FFSG II) to the Early to Middle Holocene, and the upper sediments east of core MC30 from the last millennium (FFSG I) to the earlier Late Holocene. Hence, our study reveals that care must be taken when chronologically classifying fluvial sediments even within one river system just based on their stratigraphical-geomorphological positions and/or sediment properties (cf. Kolb et al., 2016; Khosravichenar et al., 2020).

5.2. *Holocene overbank sedimentation phases in the Weiße Elster floodplain*

Based on the stratigraphical contexts and numerical ages, our investigations in the middle Weiße Elster floodplain revealed several main phases of Holocene overbank sedimentation. In order to exclude local overbank sedimentation just due to river-intrinsic effects (Khosravichenar et al., 2020), these phases were only assigned in case that (i) they were detected at least in two different transects, or (ii) they were detected in just one transect but their sediments cover larger areas (Fig. 7). However, we did not systematically compare the sediment thicknesses from different phases with each other, since these cannot be regarded as proxies for the intensities of sediment input to the floodplain due to regular sediment remobilization and redeposition (von Suchodoletz et al., 2022):

(i) The first phase occurred between ca. 11 and 10 ka during the Early Holocene, and its sediments were found in Salsitz and Meilitz. In Salsitz they obviously form a thin and incomplete cover in the floodplain, and due to the large errors of the luminescence ages their dating was only very approximate. However, a radiocarbon age of underlying peat from a paleochannel of 11.2–10.8 cal. ka BP gave a *terminus post quem* for these sediments. The fact that no overprinting paleosol could be detected can possibly be explained with its erosion immediately prior to new sediment aggradation, or with the observed strong overprinting by iron-manganese dynamics due to groundwater fluctuations. In Meilitz, sediments from this phase form an abandoned inorganic channel fill, and incorporated charcoal was dated to 10.4–10.2 cal. ka BP.

(ii) The second phase occurred around 9 ka during the final Early Holocene. Its sediments were only found in Trebnitz, forming a several decimeters thick continuous layer over >100 m along the transect. Their age was bracketed by the radiocarbon age of 9.5–9.3 cal. ka BP from the underlying peat, and the lowest radiocarbon age of bulk organic matter from the overprinting "Black Floodplain Soil" of 7.4–7.3 cal. ka BP. Embedded charcoal from these sediments was dated to 9.5–9.3 cal. ka BP, what could suggest that fluvial sedimentation relatively abruptly interrupted peat growth.

(iii) The third phase occurred between ca. 7.7 and 6.5 ka during the Middle Holocene, and was mainly found in Salsitz and Meilitz and with very low intensity also in Trebnitz. In Salsitz, its sediments form a several decimeters thick layer in the central floodplain. Embedded charcoal gave ages of 7.7–7.6 and 6.9–6.7 cal. ka BP, and bulk organic matter from overprinting paleosol S-PS-3 ages of 6.2–6.0 cal. ka BP. In contrast, the luminescence ages encompassing this period show rather large errors. In Meilitz, remains of these several decimeters thick sediments are only found in the easternmost floodplain, and embedded charcoal was dated to 6.7–6.5 cal. ka BP. Similar with Salsitz, a luminescence age encompassing this period shows a rather large error. In Trebnitz very slow fine-grained fluvial background sedimentation was observed during this time, whereof the sediments were immediately overprinted by the formation of the "Black Floodplain Soil".

(iv) The fourth phase occurred between ca. 4.2 and 3.5 ka during the early Late Holocene, and its sediments were found in Salsitz and Trebnitz. In Salsitz, these several decimeters thick sediments cover large parts of the western floodplain. Charcoal from their base was dated to 4.4–4.2 cal. ka BP, and a luminescence sample to 3.9–3.5 ka. Largely missing sediments from preceding phase (iii) indicate strong lateral erosion during this phase (von Suchodoletz et al., 2022). Although charcoal from their uppermost part was dated to 3.1–2.9 cal. ka BP suggesting a longer duration of this phase, this single age could potentially also be linked with overprinting paleosol S-PS-1. Hence, we did not prolong phase (iv) until that time. In Trebnitz, the several decimeters thick relatively coarse-grained sediments of this phase (Fig. 4c) indicate high-energy fluvial dynamics. Charcoal from their base was dated to 4.3–4.1 cal. ka BP, and charcoal from their upper part to 3.8–3.6 cal. ka BP.

(v) The fifth phase occurred between ca. 2.8 and 2.2 ka during the middle Late Holocene, and its sediments were found in Salsitz and Meilitz. In Salsitz, its several decimeters thick sediments in the central floodplain overlie Middle Holocene sediments of phase (iii), and embedded charcoal was dated to 2.7–2.5 cal. ka BP. Overlying sediments, separated from these sediments by weak paleosol S-SP-2, indicate continued fluvial sedimentation after a short sedimentation break. Accordingly, within their relatively large errors the luminescence ages from these upper sediments encompass the same period. In Meilitz, several decimeters thick sediments from this phase in the easternmost floodplain overlie sediments of phase (iii) or basal gravels. Their luminescence ages range between ca. 2.6 and 1.6 ka, however, given that only one of four ages is <2 ka this could also be derived from a very local sedimentation or form an outlier. Hence, phase (v) was not prolonged until this time. Largely missing sediments from preceding phase (iii) in Meilitz indicate strong lateral erosion (von Suchodoletz et al., 2022).

(vi) The sixth phase, occurring around 1 ka, was only found in Salsitz during our study where its some decimeters thick sediments were dated to 0.8–0.9 ka. However, several decimeters thick overbank sediments, archaeologically dated between around 1.2 and 0.8 ka, were formerly detected in Pegau (Tinapp et al., 2008) located downstream from our study area (location see Fig. 1b). Hence, this phase seems to be a larger-scale rather than a local phenomenon.

Intensive fluvial aggradation and erosion occurred during the last centuries, and weak paleosols within the sequences indicate short-term interruptions of fluvial sedimentation. However, caused by dating uncertainties, it was rather difficult to chronologically subdivide this period. Hence, the chronological ranges of the two identified sub-periods should be considered with caution:

(vii) The seventh phase, largely occurring during the first half of the last millennium, was found in all transects. A luminescence age of 0.6 ± 0.1 ka was obtained from several decimeters thick sediments in the western part of transect Salsitz, resembling several ages from decimeters-thick sediment packages in Trebnitz and Meilitz. In the eastern part of the Trebnitz floodplain, their ages varied between 0.7 ± 0.1 and 0.4 ± 0.04 ka, and (weak) paleosols indicate at least one short interruption of sedimentation. In Meilitz, sediments from this phase were dated to 0.5 ± 0.1 ka, forming the lower part of the fine-grained sediments in the western floodplain. In both Trebnitz and Meilitz older sediments were largely eroded, indicating strong lateral erosion during this phase (von Suchodoletz et al., 2022).

(viii) The eighth phase, occurring during the second half of the last millennium, was found in all transects. Strong erosion of older sediments in Salsitz and Trebnitz indicates strong lateral erosion (von Suchodoletz et al., 2022). The ages of this phase range between 0.5 and 0.3 cal. ka BP and 0.2 ± 0.02 ka. However, its lower chronological limit could be given by the age of 0.3–0 cal. ka BP (Fig. 3a), and the upper limit by the fact that historic maps do not show strong lateral migrations of the river courses at all sites since about 1800 CE (von Suchodoletz et al., 2022). Hence, this phase obviously occurred between ca. 0.35 and 0.2 ka.

As mentioned above, former studies about overbank deposition in the Weiße Elster floodplain largely lacked numerical dating. Hence, archaeological dating and sparse numerical ages often resulted in relatively long and hence overestimated possible time frames for the bracketed overbank sedimentation phases (Fuhrmann, 1999; Tinapp et al., 2008), or coincidences between sedimentation and human settlement phases were assumed (Tinapp, 2003). This often hinders a comparison with our overbank sedimentation phases. Only in some cases numerical or archaeological ages allowed a precise chronological classification of formerly detected sedimentation phases, allowing a direct comparison with our study (Fig. 7; site locations see Fig. 1b): As mentioned above, at site Pegau archaeological dating bracketed a phase of overbank sedimentation between ca. 1.2 and 0.8 ka (Tinapp et al., 2008), encompassing phase (vi). Furthermore, at site Merseburg-Ost the oldest overbank deposits were chronologically bracketed between 7.8 ± 0.1 cal. ka BP (underlying peat) and 6.5 ± 0.6 cal. ka BP (overprinting paleosol) (Litt et al., 1987), coinciding with our phase (iii). Furthermore, organic material from fine-grained sediments in Zwenkau was dated to 8.2–8.0 cal ka BP, falling between our phases (ii) and (iii). Altogether, the rather incomplete patterns of overbank sedimentation at the studied sites in the Weiße Elster floodplain (Fig. 7) underline the need to study several sites within one river system to understand its former fluvial dynamics (Faust and Wolf, 2017; Khosravichenar et al., 2020).

5.3. *Possible external controls of Holocene overbank sedimentation in the Weiße Elster floodplain*

To obtain information about possible natural or human controls of overbank sedimentation phases in the Weiße Elster floodplain, we compared these with our former settlement pattern in the catchment, as well as with paleoclimatic and paleoenvironmental data. Unfortunately, such regional data are either fragmentary, do not contain paleoclimatic information that seems useful in our context, and/or only encompass

short periods (Litt, 1992; Wennrich et al., 2005; Breitenbach et al., 2019). Hence, next to a rather short-term record of Late Holocene Central European summer precipitation we had to use complete and longer-term Holocene records from other Central European regions, i.e., the Alpine area and NE Germany/NW Poland, that were complemented by global paleoclimatic information. However, the whole of Central Europe is located within the mid-latitude European westerlies zone. Hence, despite some regional differences, large-scale climatic and environmental fluctuations and trends recorded in other Central European sub-regions should have been similar with those in our study area (Mann, 2002; Magny, 2004; Roberts et al., 2018; Pleskot et al., 2020).

In the following, we discuss Holocene overbank sedimentation phases within the Weiße Elster floodplain against possible external natural and human drivers and in comparison with other regional studies (Fig. 8):

(i) Overbank sedimentation between ca. 11 and 10 ka in Salsitz and Meilitz occurred prior to Neolithic settlement. However, it coincided with higher lake levels in the northwestern pre-Alps that were largely concomitant with low temperatures in the North Atlantic and indicate more humid conditions in Central Europe (Magny, 2004). Likewise, also in the Elbe floodplain overbank deposition was observed for that time (Tinapp et al., 2023; location see Fig. 1b).

(ii) Pre-Neolithic overbank sedimentation around 9 ka was only recorded in Trebnitz. During this phase no higher lake levels were recorded in the northwestern pre-Alps (Magny, 2004). However, a conspicuous charcoal layer within our sediments from this period (Figs. 4c, 5f) suggests a link of fluvial sedimentation with local fire activity, impacting the local vegetation cover. Accordingly, a pollen record from the lowest Weiße Elster floodplain (Litt, 1992; same location as Litt et al., 1987) and from a former wet depression near Kieritzsch in the lower Weiße Elster catchment (site described in Kretschmer and Viol, 2020) (both locations see Fig. 1b) indicate a regional dominance of relatively easily burning *pinus* trees until the Atlantic period. Likewise, a charcoal record from NE Germany/NW Poland indicates generally elevated Early Holocene fire activity in Central Europe that decreased since about 9 ka (Dietze et al., 2018). Radiocarbon dating from underlying peat of 9.5–9.3 cal. ka BP in core TC2 gives a *terminus post quem* for overbank sedimentation. Hence, similar with a study from a *pinus*-dominated region in NE

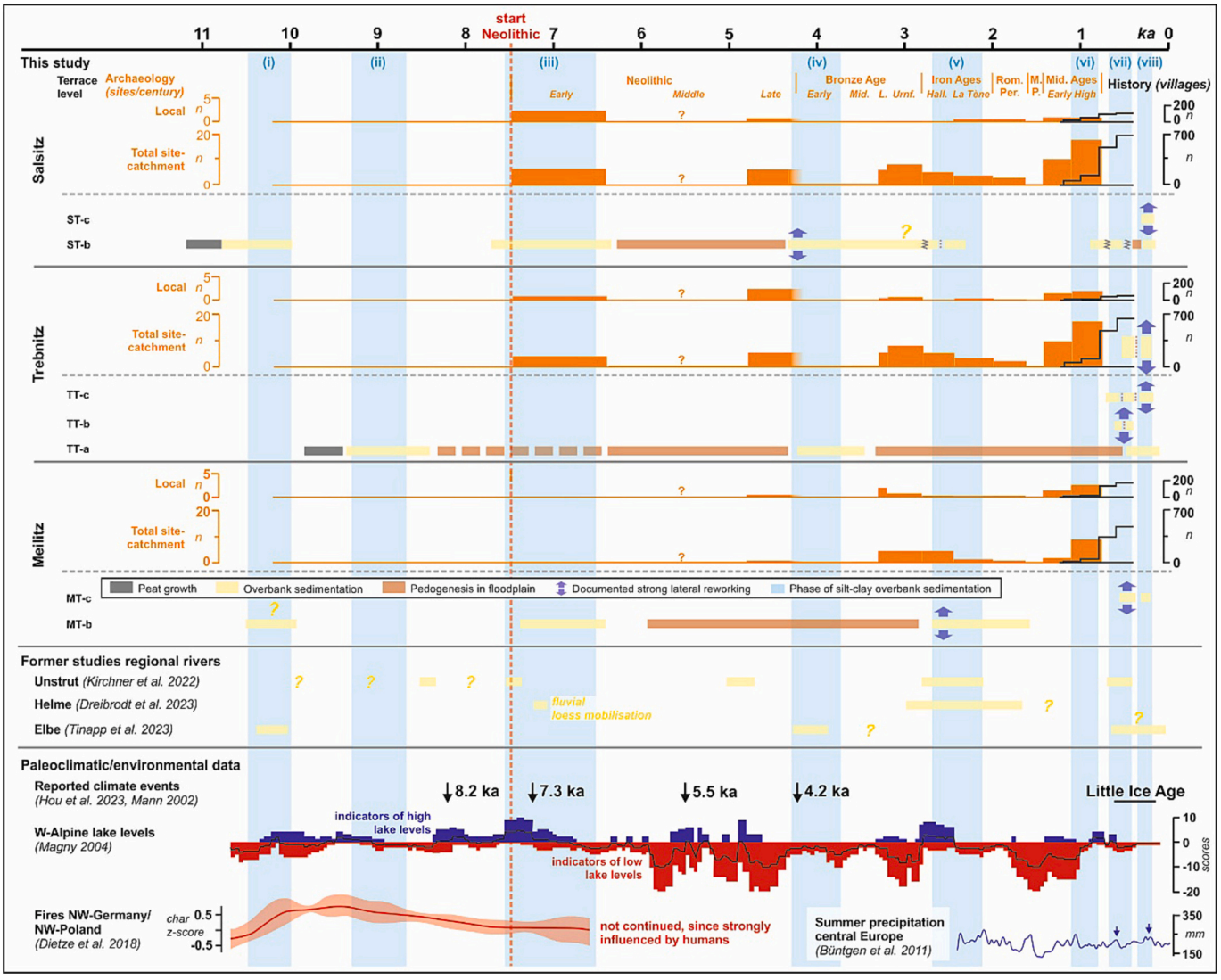

Fig. 8. Comparison of phases of overbank sedimentation (blue shaded) and lateral reworking in the Weiße Elster floodplain with former settlement patterns, former studies about regional rivers (locations see Fig. 1a) and Central European paleoclimatic/environmental data. We show different graphs of former settlement activity based on archaeology and history, since these are based on different methods. (For interpretation of the references to color in this figure legend, the reader is referred to the web version of this article.)

Germany (Dreibrodt et al., 2010) this theoretically also allows a link of fire activity with drier conditions around 9.5 ka.

(iii) Overbank sedimentation between ca. 7.7 and 6.5 ka in Salsitz and Meilitz, and with very low amounts also in Trebnitz, occurred during the regional Early Neolithic. Both the local and total site sub-catchments of Salsitz featured intensive settlement activity, whereas Fig. 8 does not show such activity for Meilitz. However, several stray finds of Neolithic age, partly also specified to the Early Neolithic, were recorded for the latter whereof the unspecified finds are not shown in Fig. 8 (Table 4; Miera et al., 2022). Hence, Early Neolithic human influence of unknown kind and intensity is also possible for site Meilitz. Furthermore, phase (iii) coincided with more humid conditions in Central Europe during the 7.3 ka global climatic event (Magny, 2004; Hou et al., 2023). Hence, we suggest the interplay of both human and climatic causes for significant overbank sedimentation during that phase: During more humid conditions the regional vegetation was partly destabilized by Early Neolithic human activity, allowing a relatively easy sediment transport from the slopes to the floodplain. Concomitantly, fluvial loess redeposition was observed in the Helme floodplain, and fine-grained channel filling at the Unstrut River (Dreibrodt et al., 2023, Kirchner et al., 2022; locations see Fig. 1a).

(iv) Coarser-grained and hence higher-energy overbank sedimentation (Fig. 4c) occurred ca. 4.2–3.5 ka in Salsitz and Trebnitz during the Early Bronze Age, largely representing a settlement gap within the study area. However, intensive and medium settlement activity during the preceding Late Neolithic was recorded in the total and local site sub-catchments of Salsitz, respectively, and intensive settlement activity in both the total and local site sub-catchments of Trebnitz. Phase (iv) coincided with the global 4.2 ka climatic event that was especially well expressed in lower latitudes such as the Mediterranean Basin (Bini et al., 2019), but also by a decreasing number of low lake level indicators in the northwestern pre-Alps (Magny, 2004) and higher snowmelt fluxes during spring in Poland (Pleskot et al., 2020). Hence, higher peak flows of the Weiße Elster due to higher spring snowmelt (Fig. 1c) could not only explain the observed higher-energy fluvial sedimentation (Fig. 4c), but also intensive river channel migration in Salsitz (Kleinhans and van den Berg, 2011). Apparently, high sediment delivery during that time can possibly be explained by a sediment cascade, i.e. slope material that was primarily eroded during preceding intensive Late Neolithic settlement was transported to the floodplain only during the following more humid period (Fuchs et al., 2011). Concomitantly, overbank sedimentation also resumed in the Elbe floodplain (Tinapp et al., 2023).

(v) Overbank sedimentation between ca. 2.8 and 2.2 ka in Salsitz and Meilitz coincided with relatively intensive Iron Age settlement activity in all total, and with low to medium settlement intensities in all local site sub-catchments. Furthermore, overbank sedimentation was also preceded by intensive settlement activity during the Urnfield period in all total site sub-catchments. Additionally, this phase coincided with humid conditions in the northwestern pre-Alps (Magny, 2004), and with relatively high summer precipitation in Central Europe (Büntgen et al., 2011). Hence, we suggest that during this phase the temporal coincidence of intensive human activity and more humid conditions caused intensive overbank sedimentation. Furthermore, strong lateral erosion in Meilitz, recognized by the large-scale removal of overbank sediments from phase (iii), indicates high peak flows during this time. Although chronologically partly extending beyond our sedimentation phase, concomitant overbank sedimentation was also found in the Unstrut and Helme floodplains (Kirchner et al., 2022; Dreibrodt et al., 2023).

(vi) Overbank sedimentation around 1 ka in Salsitz, and in formerly studied site Pegau (Tinapp et al., 2008; location Fig. 1b) in the lower Weiße Elster floodplain, coincided with the High Middle Ages. According to the archaeological and written historical record (Figs. 8, 6b), in most site-subcatchments this time was characterized by significantly increasing settlement activities compared with the preceding Early Middle Ages. Additionally, the later part of this phase partly coincided with humid conditions in the pre-Alps (Magny, 2004). Hence, also for this phase we suggest that intensive human activity paralleled by more humid conditions caused intensive overbank sedimentation. No lateral erosion was observed during this phase.

(vii) Overbank sedimentation between ca. 0.7 and 0.4 ka (ca. 1300–1600 CE), recorded at all three sites, encompassed the early Little Ice Age (LIA; Mann, 2002). Although showing a relative increase of low lake level indicators in the northwestern pre-Alps indicating generally less humid conditions (Magny, 2004), summer precipitation in Central Europe peaked during this time (Büntgen et al., 2011). Accordingly, relatively coarse-grained overbank sedimentation (Fig. 4f) and strong lateral erosion in Trebnitz indicate high peak flows during this phase. Concomitantly, the written historical record shows a strong increase of village foundations at the beginning of this phase (Fig. 6c). Hence, also this phase of intensive overbank sedimentation was possibly caused by intensive human activity in parallel with more humid conditions. Similarly, also the Unstrut River showed overbank sedimentation during that time (Kirchner et al., 2022), and tentatively also the Elbe River (Tinapp et al., 2023). Generally, this time is known as a period of high climatic instability in Central Europe, also including catastrophic geomorphic events such as that linked with the Magdalenian Flood of 1342 CE also recorded the Weiße Elster catchment (Fütterer, in press). Accordingly, for this time also Rumsby and Macklin (1996) report increased fluvial activity with alluviation and increased lateral migration for several rivers in Northwestern Europe.

(viii) Overbank sedimentation between ca. 0.35 and 0.2 ka (ca. 1650–1800 CE), recorded at all three sites, occurred during the final LIA. Whereas the northwestern pre-Alps did not show increasing humidity, next to generally colder temperatures this time was characterized by higher summer precipitation in Central Europe (Büntgen et al., 2011). Accordingly, intensive and relatively coarse-grained fluvial sedimentation (Fig. 4a, b, c, d, f) and lateral erosion in Salsitz and Trebnitz indicate high peak flows during that phase. No settlement record of the study area is available for this time, however, following a population reduction due to the Thirty Year's War 1618–1648 CE the German population, and possibly also that of the study area, strongly increased again (Poschlod, 2015). Hence, also during this phase more humid conditions coincided with an increasing population, what possibly caused intensive overbank sedimentation. During this time, conceivably, the Elbe showed fluvial sedimentation as well (Tinapp et al., 2023). Likewise, after a calmer period between about 1550–1650 CE, Rumsby and Macklin (1996) observe increased fluvial activity with alluviation and channel aggradation for several rivers in Northwestern Europe, however, that activity period also extended beyond 1800 CE. Based on our radiocarbon ages, this phase did obviously not encompass the Thuringian Deluge of 1613 (Ohlig, 2013), but includes high-intensity events such as the ice flood in 1784 that is also documented in the Weiße Elster catchment (Fütterer, in press).

On the one hand, some of our overbank sedimentation phases did not coincide with high settlement activity in the sub-catchments of the affected sites, whereas others do (Fig. 8). Hence, unlike most former studies mainly from western and southern Central Europe overbank sedimentation was not necessarily (directly) linked with human clear-

cutting of the protecting vegetation cover (Starkel et al., 2006; Fuchs et al., 2011; Notebaert et al., 2011; Houben et al., 2013; Stolz et al., 2013). On the other hand, all but phase (ii) coincided with documented more humid periods linked with generally colder conditions in the North Atlantic realm (Mann, 2002; Magny, 2004), and/or with periods of increased summer precipitation in Central Europe (Büntgen et al., 2011). Hence, we suggest an intricate interplay between natural and human controls for overbank sedimentation in the Weiße Elster floodplain:

- The flooding events needed for overbank sedimentation were possibly linked with extreme peak flows either caused by more discharge due to high snowmelt fluxes and/or ice jams during spring (Pleskot et al., 2020; Fütterer, in press), or with high summer precipitation possibly linked with Vb weather types (Büntgen et al., 2011; Nissen et al., 2013) (discharge regime of the Weiße Elster see Fig. 1c).
- Although also some kind of Mesolithic influence on the Central European sediment dynamics is discussed (Bos and Urz, 2003; Dotterweich et al., 2013), similar with Dreibrodt et al. (2010) the necessary sediment mobilization from the slopes to the floodplain most certainly had natural causes during pre-Neolithic phases (i) and (ii). Accordingly, for phase (ii), occurring during a period of generally increased fire activity in Central Europe (Dietze et al., 2018; Fig. 8), fire activity in the surroundings of the affected site Trebnitz is documented in our sediments (Figs. 4c, 5f). Similarly, despite missing direct evidence local fire activity could also have played a role for phase (i), since the Central German lowlands showed a prolonged dominance of relatively easily burning *pinus* trees until the Atlantic period (Litt, 1992, unpublished results from site Kieritzsch). Furthermore, Early and Middle Holocene land snail data from sediment archives in Central Germany show many species preferring open vegetation in the drier lowlands, and only in the higher altitudes of the neighboring mid-mountain ranges the proportions of typical forest species increased during that time (Mania, 1972; Fig. 9). The concomitant dominance of tree (*pinus*) over non-arboreal pollen in Zöschen (Litt, 1992) and Kieritzsch (unpublished results) from the same area can possibly be explained by different spatial scales of both proxies: Whereas pollen is distributed by wind over several kilometers reflecting the regional vegetation (Schwark et al., 2002), land snails only have spatial ranges of <100 m giving local information (Edworthy et al., 2012; Parkyn et al., 2014). Hence, prior to Neolithic settlement the drier regions of Central Germany, possibly also including our studied sites and parts of their subcatchments with current precipitation <600 mm/a (Fig. 9), obviously also showed interspersed non-forested habitats. Our study area was partly intensively settled since the Early Neolithic. Accordingly, since that time most overbank sedimentation phases temporally coincided with human settlement. However, for phase (iv) we observe a time lag between intensive settlement and following overbank sedimentation. As mentioned above this could possibly be linked with a sediment cascade, i.e., slope material that was

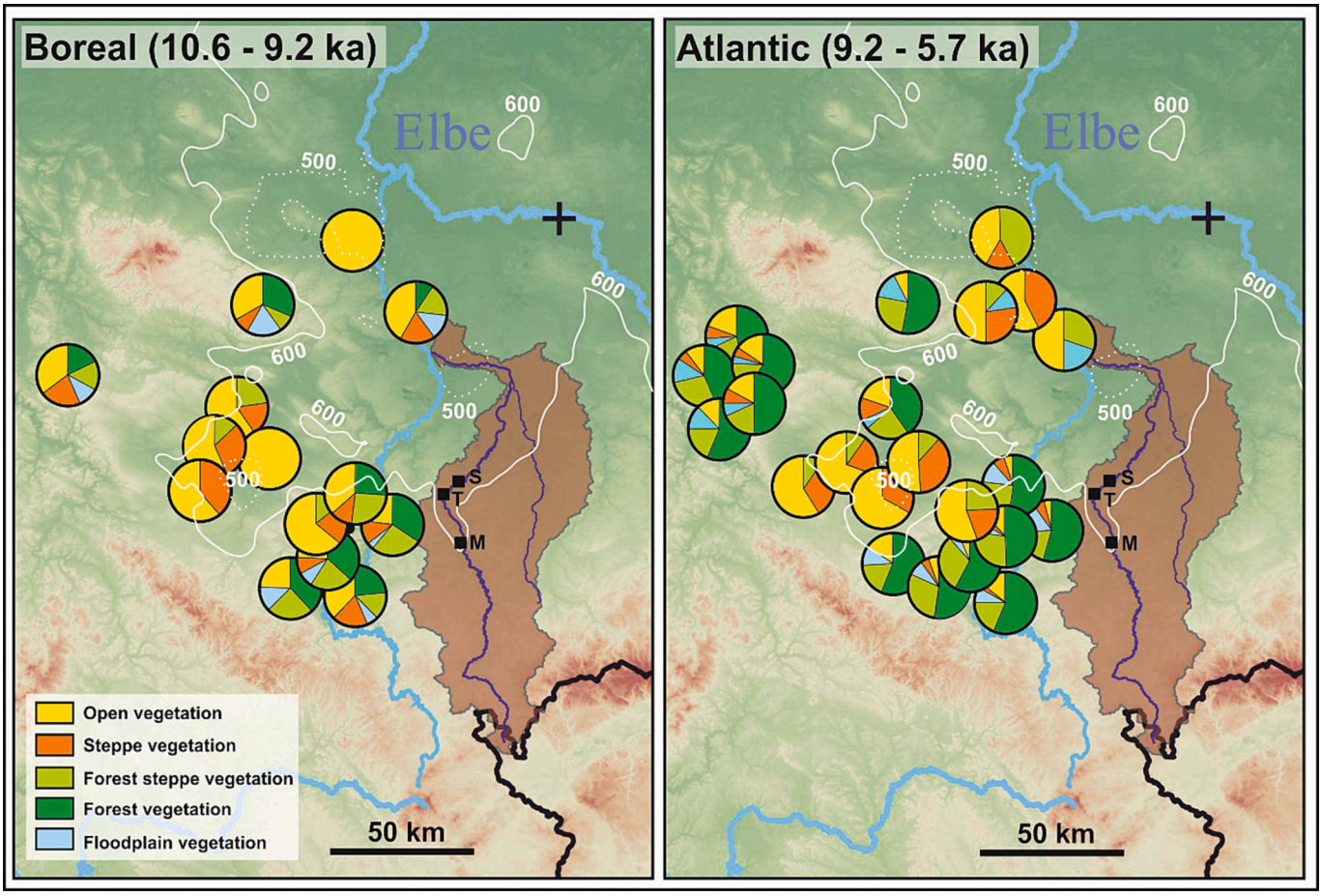

Fig. 9. Results of land snail analyses in Central Germany (Mania, 1972), and current mean annual precipitation patterns. Furthermore, the Weiße Elster catchment (brown) with our studied transects (S = Salsitz, T = Trebitz, M = Meilitz) is shown. The 500 mm/a (hatched) and 600 mm/a (solid) isohyets of annual precipitation are based on data of the German Meteorological Service (DWD). The topography of the maps is based on SRTM 90 m v. 4.1 data, and the chronology of the Boreal and Atlantic periods was taken from Kaiser et al. (2023). (For interpretation of the references to color in this figure legend, the reader is referred to the web version of this article.)

primarily eroded during intensive Late Neolithic human settlement, a period with strongly increased low lake level indicators in the northwestern pre-Alps indicating drier conditions (Magny, 2004), was transported into the floodplain only during the following more humid period (Fuchs et al., 2011). Finally, during the Late Holocene overbank sedimentation phases larger amounts of fine-grained material already existed in the floodplain. Hence, next to direct sediment input from the slopes, indicated by systematically decreasing weathering degrees of the sediments with time (upwards mostly decreasing Rb/Sr-ratios in Fig. 4), also in-river reworking of older sediments must have played a role for overbank sedimentation what is demonstrated by signs of strong lateral reworking since phase (iv).

6. Conclusions

We compared our quite well-dated Holocene overbank deposits in the Weiße Elster floodplain with a spatio-temporally exceptionally well-resolved regional former settlement record, as well as with paleoclimatic and paleoenvironmental data from Central Europe. This dataset allowed unprecedented insights into possible natural and human drivers of Holocene overbank sedimentation in a Central European meso-scale river system. Unlike most former studies from Western and Central Europe, our data suggest that the overbank sedimentation phases were obviously not necessarily linked with human activities in the affected site sub-catchments, but were also linked with natural factors leading to sediment mobilization from the slopes into the floodplain. On the one hand, this difference with most former studies could possibly be explained by previously often limited numerical dating of the fluvial sediments, as well as by largely missing spatio-temporally well-resolved settlement records from the studied sub-catchments, hindering a precise temporal link of fluvial sedimentation with former human settlement. On the other hand, this difference could possibly also be explained by a higher natural sensitivity of the landscape dynamics in the Central German lowlands towards external controls. This could be caused by the regional subcontinental climate, leading to a more open natural vegetation cover compared with most former study areas located in climatically more oceanic areas.

However, the fluvial and sediment dynamics of the Weiße Elster river catchment are rather complex, and despite a relatively large number of numerical ages our age model partly show rather large uncertainties due to methodical issues of the applied dating methods. Furthermore, the lack of well-resolved regional paleoclimatic and paleoenvironmental data makes the comparison of our overbank sedimentation phases with natural factors rather approximate. Hence, although our study represents a large step forward with respect to former studies, also for the Weiße Elster catchment the intricate interplay of natural and human causes for overbank sedimentation is far from being well understood. Furthermore, for more insights into these processes detailed research on the Holocene slope sediment dynamics within the Weiße Elster catchment is needed, allowing to understand slope-floodplain coupling including possible sediment cascades. Such investigations are currently underway.

CRediT authorship contribution statement

Hans von Suchodoletz: Conceptualization, Data curation, Formal analysis, Funding acquisition, Investigation, Methodology, Project administration, Visualization, Writing – original draft, Writing – review & editing. **Azra Khosravichenar:** Data curation, Investigation, Writing – original draft, Writing – review & editing. **Pierre Fütterer:** Conceptualization, Data curation, Formal analysis, Funding acquisition, Investigation, Methodology, Writing – original draft, Writing – review & editing. **Christoph Zielhofer:** Conceptualization, Data curation, Funding acquisition, Methodology, Project administration, Writing – original draft, Writing – review & editing. **Birgit Schneider:** Data curation, Formal analysis, Methodology, Writing – original draft, Writing – review & editing. **Tobias Sprafke:** Data curation, Formal analysis, Investigation, Methodology, Visualization, Writing – original draft, Writing – review & editing. **Christian Tinapp:** Conceptualization, Data curation, Methodology, Writing – original draft, Writing – review & editing. **Alexander Fülling:** Formal analysis, Investigation, Methodology, Writing – original draft, Writing – review & editing. **Lukas Werther:** Conceptualization, Data curation, Funding acquisition, Methodology, Writing – original draft, Writing – review & editing. **Harald Stäuble:** Conceptualization, Methodology, Writing – original draft, Writing – review & editing. **Michael Hein:** Methodology, Visualization, Writing – original draft, Writing – review & editing. **Ulrich Veit:** Conceptualization, Data curation, Funding acquisition, Methodology, Writing – original draft, Writing – review & editing. **Peter Ettel:** Conceptualization, Funding acquisition, Methodology, Project administration, Writing – original draft, Writing – review & editing. **Ulrike Werban:** Conceptualization, Funding acquisition, Methodology, Project administration, Writing – original draft, Writing – review & editing. **Jan Miera:** Data curation, Formal analysis, Funding acquisition, Investigation, Methodology, Project administration, Visualization, Writing – original draft, Writing – review & editing.

Declaration of competing interest

The authors declare the following financial interests/personal relationships which may be considered as potential competing interests: Hans von Suchodoletz reports financial support was provided by German Research Foundation. If there are other authors, they declare that they have no known competing financial interests or personal relationships that could have appeared to influence the work reported in this paper.

Data availability

Data will be made available on request.

Acknowledgements

This study was financially supported by the DFG-funded project ‘Imprints of rapid climate changes and human activity on Holocene hydro-sedimentary dynamics in Central Europe (loess-covered Weiße Elster model region)’ (SU491/6-1, ET20/10-1, VE117/7-1, WE5518/1-1, ZI721/13-1). Furthermore, we are indebted to Katja Pöhlmann (Leipzig) for her help during sediment sample preparation, Flavio Anselmetti for providing access to the polarizing light microscope of the Institute of Geology, University of Bern, and Johanna L. von Suchodoletz (Leipzig) for digitizing material for the figures. We thank Jef Vandenberghe and an anonymous reviewer for their helpful comments on this manuscript.

Appendix A. Supplementary data

Supplementary data to this article can be found online at https://doi.org/10.1016/j.geomorph.2024.109067.

6. References

Ahlrichs, J.J., Henkner, J., Schmidt, K., Scholten, T., Kühn, P., Knopf, T., 2018. Bronzezeitliche Siedlungsdynamiken zwischen der Baar und angrenzenden Naturräumen. In: Neumann, D., Nessel, B., Bartelheim, M. (Eds.), Bronzezeitlicher Transport: Akteure, Mittel und Wege. RessourcenKulturen 8. Tübingen University Press, Tübingen, pp. 269–303.

Autorenkollektiv, 1976. Das obere Vogtland. Ergebnisse der heimatkundlichen Bestandsaufnahme in den Gebieten von Adorf, Klingenthal, Bad Elster und Schönberg. Werte unserer Heimat 26, Berlin.

Autorenkollektiv, 1986. Plauen und das mittlere Vogtland. Ergebnisse der heimatkundlichen Bestandsaufnahme in den Gebieten Plauen-Nord, Treuen, Plauen-Süd und Oelsnitz. Werte unserer Heimat 44, Berlin.

Ballasus, H., Schneider, B., von Suchodoletz, H., Miera, J., Werban, U., Fütterer, P., Werther, L., Ettel, P., Veit, U. & C. Zielhofer (2022a): Overbank silt-clay deposition

and extensive Neolithic land-use in a Central European floodplain – coupled or decoupled? Sci. Total Environ. 806, 150858.
Ballasus, H., Suchodoletz, H., von Schneider, B., Grün, H., Heller, A., Kind, M.-S., Wroblewski, B., Wurlitzer, S. & C. Zielhofer (2022b): Hydro-sedimentary provenance analyses in the Weiße Elster catchment (Central Germany): the basic dataset. Data Brief 40, 107719.
BFN, 2012. Landschaftssteckbriefe. Bundesamt für Naturschutz, Bonn. www.bfn.de/landschaften/steckbriefe.
Bini, M., Zanchetta, G., Persoiu, A., Cartier, R., Català, A., Cacho, I., Dean, J.R., Di Rita, F., Drysdale, R.N., Finnè, M., Isola, I., Jalali, B., Lirer, F., Magri, D., Masi, A., Marks, L., Mercuri, A.M., Peyron, O., Sadori, L., Sicre, M.-A., Welc, F., Zielhofer, C., Brisset, E., 2019. The 4.2 ka BP Event in the Mediterranean region: an overview. Clim. Past 15, 555–577.
Bohn, U., Welß, W., 2003. Die potenzielle natürliche Vegetation. In: Nationalatlas Bundesrepublik Deutschland, Natur und Umwelt II: Klima, Pflanzen- und Tierwelt, vol. 3. Leibniz Institut für Länderkunde, Leipzig.
Bos, J.A.A., Urz, R., 2003. Lateglacial and early Holocene environment in the middle Lahn river valley (Hessen, central-west Germany) and the local impact of early Mesolithic people—Pollen and macrofossil evidence. Veg. Hist. Archaeobotany 12, 19–36.
Breitenbach, S., Plessen, B., Waltgenbach, S., Tjallingii, R., Leonhardt, J., Jochum, K.P., Meyer, H., Goswami, B., Marwan, N., Scholz, D., 2019. Holocene interaction of maritime and continental climate in Central Europe: new speleothem evidence from Central Germany. Glob. Planet. Chang. 176, 144–161.
Broothaerts, N., Notebaert, B., Verstraeten, G., Kasse, C., Bohncke, S., Vandenberghe, J., 2014a. Non-uniform and diachronous Holocene floodplain evolution: a case study from the Dijle catchment, Belgium. J. Quat. Sci. 29, 351–360.
Broothaerts, N., Verstraeten, G., Kasse, C., Bohncke, S., Notebaert, B., Vandenberghe, J., 2014b. Reconstruction and semi-quantification of human impact in the Dijle catchment, central Belgium: a palynological and statistical approach. Quat. Sci. Rev. 102, 96–110.
Brown, A.G., Lespez, L., Sear, D.A., Macaire, J.-J., Houben, P., Klimek, K., Brazier, R.E., van Oost, K., Pears, B., 2018. Natural vs anthropogenic streams in Europe: history, ecology and implications for restoration, river-rewilding and riverine ecosystem services. Earth Sci. Rev. 180, 185–205.
Buchty-Lemke, M., Hagemann, L., Maaß, A.-L., 2019. Floodplain chronology and sedimentation rates for the past 200 years derived from trace element gradients, organic compounds, and numerical modeling. Environ. Earth Sci. 78, 445.
Büntgen, U., Tegel, W., Nicolussi, K., McCormick, M., Frank, D., Trouet, V., Kaplan, J.O., Herzig, F., Heussner, K.-U., Wanner, H., Luterbacher, J., Esper, J., 2011. 2500 years of European climate variability and human susceptibility. Science 331, 578–582.
Buylaert, J.P., Murray, A.S., Thomsen, K.J., Jain, M., 2009. Testing the potential of an elevated temperature IRSL signal from K-feldspar. Radiat. Meas. 44, 560–565.
Crowther, J., 2003. Potential magnetic susceptibility and fractional conversion studies of archaeological soils and sediments. Archaeometry 45, 685–701.
Dietze, E., Theuerkauf, M., Bloom, K., Brauer, A., Dörfler, W., Feeser, I., Feurdean, A., Gedminiene, L., Giesecke, T., Jahns, S., Karpińska-Kołaczek, M., Kołaczek, P., Lamentowicz, M., Latałowa, M., Marcisz, K., Obremska, M., Pędziszewska, A., Poska, A., Rehfeld, K., Stančikaitė, M., Stivrins, N., Święta-Musznicka, J., Szal, M., Vassiljev, J., Veski, S., Wacnik, A., Weisbrodt, D., Wietholdt, J., Vannière, B., Słowiński, M., 2018. Holocene fire activity during low-natural flammability periods reveals scale-dependent cultural human-fire relationships in Europe. Quat. Sci. Rev. 201, 44–56.
Dotterweich, M., Kühn, P., Tolksdorf, J.F., Müller, S., Nelle, O., 2013. Late Pleistocene to Early Holocene natural and human influenced sediment dynamics and soil formation in a 0-order catchment in SW-Germany (Palatinate Forest). Quat. Int. 306, 42–59.
Dreibrodt, S., Lomax, J., Nelle, O., Lubos, C., Fischer, P., Mitusov, A., Reiss, S., Radtke, U., Nadeau, M., Grootes, P.M., Bork, H.-R., 2010. Are mid-latitude slopes sensitive to climatic oscillations? Implications from an Early Holocene sequence of slope deposits and buried soils from eastern Germany. Geomorphology 122, 351–369.
Dreibrodt, S., Langan, C.C.M., Fuchs, M., Bork, H.-R., 2023. Anthropogenic impact on erosion, pedogenesis and fluvial processes in the central European landscapes of the eastern Harz mountains forelands (Germany). Quat. Sci. Rev. 303, 107980.
Duller, G.A.T., 2003. Distinguishing quartz and feldspar in single grain luminescence measurements. Radiat. Meas. 37, 161–165.
Edworthy, A.B., Steensma, K.M.M., Zandberg, H.M., Lilley, P.L., 2012. Dispersal, home-range size, and habitat use of an endangered land snail, the Oregon forestsnail (Allogona townsendiana). Can. J. Zool. 90, 875–884.
Eggert, M.K.H., 2012. Prähistorische Archäologie: Konzepte und Methoden. UTB 2092, 4th ed. Francke, Tübingen.
Eggert, M.K.H., Samida, S., 2013. Ur- und frühgeschichtliche Archäologie. UTB 3254.. Tübingen, Francke.
Eichler, E., Walther, H., 1984. Untersuchungen zur Ortsnamenkunde und Sprach- und Siedlungsgeschichte des Gebietes zwischen mittlerer Saale und Weißer Elster. In: Deutsch-slawische Forschungen zur Namenkunde und Siedlungsgeschichte, vol. 35. De Gruyter, Berlin.
Eichler, E., Walther, H., 2001. Historisches Ortsnamenbuch von Sachsen. In: Quellen und Forschungen zur sächsischen Geschichte, vol. 21. Akademie Verlag, Berlin.
Eichler, E., Hellfritzsch, V., Richter, J., 1983. Die Ortsnamen des sächsischen Vogtlandes. Herkunft - Entwicklung - Bedeutung I. Namenbuch. In: Schriftenreihe des Vogtlandmuseums Plauen, vol. 50.
Eichler, E., Hellfritzsch, V., Richter, J., 1985. Die Ortsnamen des sächsischen Vogtlandes. Herkunft - Entwicklung - Bedeutung II. Zur Namenkunde und Siedlungsgeschichte. In: Schriftenreihe des Vogtlandmuseums Plauen, vol. 53.
Eissmann, L. (2002): Quaternary geology of eastern Germany (Saxony, Saxon–Anhalt, South Brandenburg, Thuringia), type area of the Elsterian and Saalian Stages in Europe. Quat. Sci. Rev. 21, 1275–1346.
Erkens, G., Dambeck, R., Volleberg, K.P., Bouman, M.T.I.J., Bos, J.A.A., Cohen, K.M., Wallinga, J., Hoek, W.Z., 2009. Fluvial terrace formation in the northern Upper Rhine Graben during the last 20000 years as a result of allogenic controls and autogenic evolution. Geomorphology 103, 476–495.
Faust, D., Wolf, D., 2017. Interpreting drivers of change in fluvial archives of the Western Mediterranean - a critical view. Earth Sci. Rev. 174, 53–83.
Fuchs, M., 2001. Die OSL-Datierung von Archäosedimenten zur Rekonstruktion anthropogen bedingter Sedimentumlagerung. Ibidem, Stuttgart.
Fuchs, M., Will, M., Kunert, E., Kreutzer, S., Fischer, M., Reverman, R., 2011. The temporal and spatial quantification of Holocene sediment dynamics in a meso-scale catchment in northern Bavaria, Germany. The Holocene 21, 1093–1104.
Fuhrmann, R., 1999. Klimaschwankungen im Holozän nach Befunden aus Fluß- und Bachablagerungen Nordwestsachsens und angrenzender Gebiete. Altenburger Naturwissenschaftliche Forschungen 11, 3–41.
Fuhrmann, R., 2005. Klimaschwankungen im Holozän nach Befunden aus Talsedimenten Mitteldeutschlands. Mauritiana 19, 289–304.
Fütterer, P., 2016. Wege und Herrschaft. Untersuchungen zu Raumerschließung und Raumerfassung in Ostsachsen und Thüringen im 10. und 11. Jahrhundert. In: Palatium Studien zur Pfalzenforschung in Sachsen-Anhalt, vol. 2. Akademie Verlag, Regensburg.
Fütterer, P., 2024. Alle Wetter - Zum Einfluss von Hochwassern auf Mensch und Raum am Beispiel der Weißen Elster. In: Schimpff, V., Hummel, A., Beier, H.-J. (Eds.), 1122–2022. Neunhundert Jahre Plauen und der Dobnagau. Das Vogtland im Hoch- und Spätmittelalter, Beiträge zur Frühgeschichte und zum Mittelalter Ostthüringens, vol. 13. Beier and Beran (in press, Langenweißbach).
Galbraith, R.F., Roberts, R.G., Laslett, G.M., Yoshida, H., Olley, J.M., 1999. Optical dating of single and multiple grains of quartz from Jinmium Rock Shelter, Northern Australia: part I: experimental design and statistical models. Archaeometry 41, 339–364.
Gebica, P., Jacyszyn, A., Krapiec, M., Budek, A., Czumak, N., Starkel, L., Andrejczuk, W., Ridush, B., 2016. Stratigraphy of alluvia and phases of the Holocene floods in the valleys of the Eastern Carpathians foreland. Quat. Int. 415, 55–66.
Haase, D., Fink, J., Haase, G., Ruske, R., Pécsi, M., Richter, H., Altermann, M., Jäger, K.-D., 2007. Loess in Europe - its spatial distribution based on a European loess map, scale 1:2,500,000. Quat. Sci. Rev. 26, 1301–1312.
Hall, S.A., Periman, R.D., 2007. Unusual Holocene alluvial record from Rio del Oso, Jemez Mountains, New Mexico: Paleoclimatic and archeologic significance. New Mexico Geological Society Guidebook, 58th Field Conference. Geology of the Jemez Mountains Region II, 459–468.
Händel, D., 1967. Das Holozän in den nordwestsächsischen Flußauen. Hercynia N.F. 4, 152–198.
Händel, D., 1969. Auelehmsedimentation und Laufentwicklung in den Auen der Weißen Elster und Pleiße (Westsachsen). Petermanns Geogr. Mitt. 113, 16–21.
Heynowski, R., Reiß, R. (Eds.), 2010. Atlas zur Geschichte und Landeskunde von Sachsen. Sächsische Akademie der Wissenschaften zu Leipzig, Leipzig.
Hilbig, O., 1993. Zur Besiedlungsgeschichte im Gebiet um den Göttwitzer See, Kr. Grimma (Sachsen). Arbeits- und Forschungsberichte zur sächsischen Bodendenkmalpflege 36, 7–65.
Hinz, M., 2014. Neolithische Siedlungsstrukturen im südöstlichen Schleswig-Holstein: Dynamik in Landschaft und Besiedlung. In: Frühe Monumentalität und soziale Differenzierung, vol. 3. Habelt, Bonn.
Hoffmann, T., Erkens, G., Cohen, K.M., Houben, P., Seidel, J., Dikau, R., 2007. Holocene floodplain sediment storage and hillslope erosion within the Rhine catchment. The Holocene 17, 105–118.
Holliday, V.T., Gartner, W.G., 2007. Methods of soil P analysis in archaeology. J. Archaeol. Sci. 34, 301–333.
Hou, M., Wu, W., Cohen, D.J., Zeng, Z., Huang, H., Zheng, H., Ge, Q., 2023. Detection of a mid-Holocene climate event at 7.2 ka BP based on an analysis of globally-distributed multi-proxy records. Paleogeography, Palaeoclimatology, Palaeoecology 618, 111525.
Houben, P., Schmidt, M., Mauz, B., Stobbe, A., Lang, A., 2013. Asynchronous Holocene colluvial and alluvial aggradation: a matter of hydrosedimentary connectivity. The Holocene 23, 544–555.
Hürkamp, K., Raab, T., Völkel, J., 2009. Lead pollution of floodplain soils in a historic mining area - age, distribution and binding forms. Water Air Soil Pollut. 201, 331–345.
IUSS Working Group WRB, 2022. World Reference Base for Soil Resources. International Soil Classification System for Naming Soils and Creating Legends for Soil Maps, 4th edition. International Union of Soil Sciences, Vienna, Austria.
Jain, M., Murray, A.S., Bøtter-Jensen, L., 2004. Optically stimulated luminescence dating: how significant is incomplete light exposure in fluvial environments? Quaternaire 15, 143–157.
Joseph, H., Porada, H.T. (Eds.), 2006. Das nördliche Vogtland um Greiz. Eine landeskundliche Bestandsaufnahme im Raum Greiz, Weida, Berga, Triebes, Hohenleuben, Elsterberg, Mylau und Netzschkau. Landschaften in Deutschland, Werte der deutschen Heimat, vol. 68. Köln/Weimar/Wien.
Kahl, W., 2010. Ersterwähnung Thüringer Städte und Dörfer. Ein Handbuch, Bad Langensalza.
Kaiser, K., Theuerkauf, M. & F. Hieke (2023): Holocene forest and land-use history of the Erzgebirge, central Europe: a review of palynological data. E & G – Quaternary Science Journal 72, 127–161.

Kenzler, H., 2012. Die hoch- und spätmittelalterliche Besiedlung des Erzgebirges. Strategien zur Kolonisation eines landwirtschaftlichen Ungunstraumes. In: Bamberger Schriften zur Archäologie des Mittelalters und der Neuzeit, vol. 4 (Bonn.
Khosravichenar, A., Fattahi, M., Amini, H., von Suchodoletz, H., 2020. The potential of small mountain river systems for paleoenvironmental reconstructions in drylands - an example from the Binaloud Mountains in northeastern Iran. Geosciences 10, 448.
Kirchner, A., Karaschewski, J., Schulte, P., Wunderlich, T., Lauer, T., 2022. Latest Pleistocene and Holocene floodplain evolution in Central Europe - insights from the Upper Unstrut catchment (NW-Thuringia/Germany). Geosciences 12, 310.
Kleinhans, M.G., van den Berg, J.H., 2011. River channel and bar patterns explained and predicted by an empirical and a physics-based method. Earth Surf. Process. Landf. 36, 721–738.
Kolb, T., Fuchs, M., Zöller, L., 2016. Deciphering fluvial landscape evolution by luminescence dating of river terrace formation: a case study from northern Bavaria, Germany. Z. Geomorphol. 60, 29–48.
Kottek, M., Grieser, J., Beck, C., Rudolf, B. & F. Rubel (2006): World map of the Köppen–Geiger climate classification updated. Meteorol. Z. 15, 259–263.
KPG, 1852. Geological Map 1:25,000, Sheet Eisenberg. Königlich-Preußischer Generalstab, Berlin.
KPGL, 1892. Geological Map 1:25,000, Sheet Weida. Königlich-Preußische Geologische Landesanstalt, Berlin.
KPGL, 1908. Geological Map 1:25,000, Sheet Zeitz. Königlich-Preußische Geologische Landesanstalt, Berlin.
KPGL, 1912. Geological Map 1:25,000, Sheet Gera. Königlich-Preußische Geologische Landesanstalt, Berlin.
Kretschmer, S., Viol, P., 2020. Vom neolithischen Siedlungsplatz bis zur neuzeitlichen Windmühle. Ausgrabungen in Sachsen 7, 20–34.
Lang, A., Hönscheidt, S., 1999. Age and source of colluvial sediments at Vaihingen-Enz, Germany. Catena 38, 89–107.
Lespez, L., Clet-Pellerin, M., Limondin-Lozouet, N., Pastre, J.-F., Fontugne, M., Marcigny, C., 2008. Fluvial system evolution and environmental changes during the Holocene in the Mue valley (Western France). Geomorphology 98, 55–70.
Lespez, L., Viel, V., Cador, J.-M., Germaine, M.-A., Germain-Vallée, C., Rollet, A.-J., Delahaye, D., 2013. Environmental dynamics of small rivers in Normandy (western France) since the Neolithic era. What lessons for today in the context of the European Water Framework Directive?. In: Proceedings of the international conference "Continental hydrosystems and European territories faced with different water Laws", July 11-13, 2011, Sion, Switzerland. Edition Friedrich Pfeil, München, pp. 71–90.
Litt, T., 1992. Fresh investigations into the natural and anthropogenically influenced vegetation of the earlier Holocene in the Elbe-Saale Region, Central Germany. Veg. Hist. Archaeobotany 1, 69–74.
Litt, T., Kohl, G., Görsdorf, J., Jäger, K.-D., 1987. Zur Datierung begrabener Böden in holozänen Ablagerungsfolgen. Jahresschrift für Mitteldeutsche Vorgeschichte 70, 177–189.
Lüttig, G., 1960. Zur Gliederung des Auelehms im Flußgebiet der Weser. Eiszeit. Gegenw. 11, 39–50.
Macklin, M.G., Lewin, J., 1993. Holocene river alluviation in Britain. Z. Geomorphol. Suppl. 88, 109–122.
Magny, M., 2004. Holocene climate variability as reflected by mid-European lake-level fluctuations and its probable impact on prehistoric human settlements. Quat. Int. 113, 65–79.
Mania, D., 1972. Zur spät- und nacheiszeitlichen Landschaftsgeschichte des mittleren Elb-Saalegebietes. Hallesches Jahrbuch für Mitteldeutsche Erdgeschichte 11, 7–36.
Mann, M.E., 2002. Little ice age. In: Munn, T. (Ed.), Encyclopedia of Global Environmental Change, vol. I. John Wiley and Sons Ltd, Chichester, pp. 504–509.
Matys-Grygar, T., 2022. Comment to Ballasus et al. (2022). Sci. Total Environ. 838, 155371.
May, J.H., Plotzki, A., Rodrigues, L., Preusser, F., Veit, H., 2015. Holocene floodplain soils along the Río Mamoré, northern Bolivia, and their implications for understanding inundation and depositional patterns in seasonal wetland settings. Sediment. Geol. 330, 74–89.
McLennan, S.M., Hemming, S., McDaniel, D.K., Hanson, G.N., 1993. Geochemical approaches to sedimentation, provenance and tectonics. Geol. Soc. Am. Spec. Pap. 285, 21–40.
Miera, J.J., Henkner, J., Schmidt, K., Fuchs, M., Scholten, T., Kühn, P., Knopf, T., 2019. Neolithic settlement dynamics derived from archaeological data and colluvial deposits between the Baar region and the adjacent low mountain ranges, southwest Germany. E & G - Quaternary Science Journal 68, 75–93.
Miera, J.J., Schmidt, K., Suchodoletz, H., von Ulrich, M., Werther, L., Zielhofer, C., Ettel, P. & U. Veit (2022): Large-scale investigations on Neolithic settlement dynamics in Central Germany based on machine learning analysis: a case study from the Weiße Elster river catchment. PLoS One 17(4): e0265835.
Mischka, D., 2007. Methodische Aspekte zur Rekonstruktion prähistorischer Siedlungen. Landschaftsgenese vom Ende des Neolithikums bis zur Eisenzeit im Gebiet des südlichen Oberrheins. In: Freiburger archäologische Studien, vol. 5. Leidorf, Rahden/Westfalen.
Murray, A.S., Wintle, A.G., 2000. Luminescence dating of quartz using an improved single-aliquot regenerative-dose protocol. Radiat. Meas. 32, 57–73.
Neumeister, H., 1964. Beiträge zum Auenlehmproblem des Pleiße- und Elstergebietes. Wissenschaftliche Veröffentlichungen des Deutschen Instituts für Länderkunde 21, 65–132.
Niller, H.-P., 1998. Prähistorische Landschaften im Lößgebiet bei Regensburg - Kolluvien, Auenlehme und Böden als Archive der Paläoumwelt. In: Regensburg: Regensburger Geographische Schriften, vol. 31.
Nissen, K., Ulbrich, U., Leckebusch, G.C., 2013. Vb cyclones and associated rainfall extremes over Central Europe under present day and climate change conditions. Meteorol. Z. 22, 649–660.
Notebaert, B., Houbrechts, G., Verstraeten, G., Broothaerts, N., Haeckx, J., Reynders, M., Govers, G., Petit, F., Poesen, J., 2011. Fluvial architecture of Belgian river systems in contrasting environments: implications for reconstructing the sedimentation history. Netherlands Journal of Geosciences – Geologie en Mijnbouw 90, 31–50.
Notebaert, B., Broothaerts, N., Verstraeten, G., 2018. Evidence of anthropogenic tipping points in fluvial dynamics in Europe. Glob. Planet. Chang. 164, 27–38.
Ohlig, C. (Ed.), 2013. Die thüringische Sintflut von 1613 und ihre Lehren für heute. Schriften der Deutschen Wasserhistorischen Gesellschaft, vol. 22 (Clausthal-Zellerfeld).
Ostritz, S., 2000. Untersuchungen zur Siedlungsplatzwahl im mitteldeutschen Neolithikum. In: Beiträge zur Ur- und Frühgeschichte Mitteleuropas, vol. 25. Beier und Beran, Weissbach.
Paetzold, D., 1992. Bemerkungen zum Siedlungsverhalten neolithischer bis latènezeitlicher Bevölkerungen zwischen Regensburg und Deggendorf. Gibt es Besiedlungsschwerpunkte in Abhängigkeit von naturräumlicher Gliederung und Bodenbeschaffenheit? Bayerische Vorgeschichtsblätter 57, 77–102.
Pankau, C., 2007. Die Besiedlungsgeschichte des Brenz-Kocher-Tals (östliche Schwäbische Alb) vom Neolithikum bis zur Latènezeit, part I. Universitätsforschungen zur prähistorischen. In: Archäologie, vol. 142. Habelt, Bonn.
Parkyn, J., Brooks, L., Newell, D., 2014. Habitat use and movement patterns of the endangered land snail thersites mitchellae (Cox, 1864)(Camenadiae). Malacologia 57, 295–307.
Pleskot, K., Apolinarska, K., Kołaczek, P., Suchora, M., Fojutowski, M., Joniak, T., Kotrys, B., Kramkowski, M., Słowiński, M., Woźniak, M., Lamentowicz, M., 2020. Searching for the 4.2 ka climate event at Lake Spore, Poland. Catena 191, 104565.
Poschlod, P., 2015. The origin and development of the Central European man-made landscape, habitat and species diversity as affected by climate and its changes - a review. Interdisciplinaria Archaeologica – Natural Sciences. Archaeology 2, 197–221.
Reimer, P.J., Austin, W.E.N., Bard, E., Bayliss, A., Blackwell, P.G., Bronk Ramsey, C., Butzin, M., Cheng, H., Edwards, R.L., Friedrich, M., Grootes, P.M., Guilderson, T.P., Hajdas, I., Heaton, T.J., Hogg, A.G., Hughen, K.A., Kromer, B., Manning, S.W., Muscheler, R., Palmer, J.G., Pearson, C., van der Plicht, J., Reimer, R.W., Richards, D.A., Scott, E.M., Southon, J.R., Turney, C.S.M., Wacker, L., Adolphi, F., Büntgen, U., Capano, M., Fahrni, S.M., Fogtmann-Schulz, A., Friedrich, R., Köhler, P., Kudsk, S., Miyake, F., Olsen, J., Reinig, F., Sakamoto, M., Sookdeo, A., Talamo, S., 2020. The IntCal20 northern hemisphere radiocarbon age calibration curve (0–55 cal kBP). Radiocarbon 62, 725–757.
Rittweger, H., 2000. The "Black Floodplain Soil" in the Amöneburger Becken, Germany: a lower Holocene marker horizon and indicator of an upper Atlantic to Subboreal dry period in Central Europe? Catena 41, 143–164.
Roberts, N., Fyfe, R.M., Woodbridge, J., Gaillard, M.-J., Davis, B.A.S., Kaplan, J.O., Marquer, L., Mazier, F., Nielsen, A.B., Sugita, F., Trondman, A.-K., Leydet, M., 2018. Europe's lost forests: a pollen-based synthesis for the last 11,000 years. Sci. Rep. 8, 716.
Rosenkranz, H., 1982. Ortsnamen des Bezirkes Gera. Der Kulturbund (Greiz).
Rumsby, B.T., Macklin, M.G., 1996. River response to the last neoglacial (the "Little Ice Age") in northern, western and central Europe. In: Branson, J., Brown, A.G., Gregory, K.J. (Eds.), Global Continental Changes: The Context of Palaeohydrology. Geological Society, London, pp. 217–233.
Schirmer, W., 1995. Valley bottoms in the late Quaternary. Zeitschrift für Geomorphologie N.F. Supplementary 100, 27–51.
Schmotz, K. (1989): Die vorgeschichtliche Besiedlung im Isarmündungsgebiet. Materialhefte zur Bayerischen Vorgeschichte, Reihe A – Fundinventare und Ausgrabungsbefunde 58. Kallmünz/Opf., Lassleben.
Schülke, A., 2011. Landschaften – eine archäologische Untersuchung der Region zwischen Schweriner See und Stepenitz. In: Römisch-germanische Forschungen, vol. 68. German-Germanic Commission, Darmstadt, Zabern.
Schwark, L., Zink, K., Lechterbeck, J., 2002. Reconstruction of postglacial to early Holocene vegetation history in terrestrial Central Europe via cuticular lipid biomarkers and pollen records from lake sediments. Geology 30, 463–466.
SLUG, 1992. Geological Overview Map of the Free State Saxony 1:400,000. Sächsisches Landesamt für Umwelt und Geologie, Freiburg.
Sprafke, T., 2016. Löss in Niederösterreich – Archiv quartärer Klima- und Landschaftsveränderungen. Würzburg University Press, Würzburg. https://opus.bibliothek.uni-wuerzburg.de/files/12778/978-3-95826-039-9_Sprafke_Tobias_OPUS_12778.pdf.
Starkel, L., Soja, R., Michczynska, D.J., 2006. Past hydrological events reflected in Holocene history of Polish rivers. Catena 66, 24–33.
Steinhof, A., Altenburg, M., Machts, H., 2017. Sample preparation at the Jena 14C laboratory. Radiocarbon 59, 815–830.
Stolz, C., Grunert, J., Fülling, A., 2013. Quantification and dating of floodplain sedimentation in a medium-sized catchment of the German uplands: a case study from the Aar Valley in the southern Rhenish Massif, Germany. Erde 144, 30–50.
Stoops, G., 2003. Guidelines for Analysis and Description of Soil Regolith in Thin Sections. Soil Science Society of America Inc., Madison (184 pp.).
Sutfin, N.A., Wohl, E.E., Dwire, K.A., 2016. Banking carbon: a review of organic carbon storage and physical factors influencing retention in floodplains and riparian ecosystems. Earth Surf. Process. Landf. 41, 38–60.
Swinnen, W., Broothaerts, N., Hoevers, R., Verstraeten, G., 2020. Anthropogenic legacy effects control sediment and organic carbon storage in temperate river floodplains. Catena 195, 104897.

Timpel, W., Spazier, I., 2014. Corpus archäologischer Quellen des 7.–12. Jahrhunderts in Thüringen, Beier & Beran, Langenweißbach.
Tinapp, C., 2003. Aktivitäts- und Stabilitätsphasen während des Holozäns im Einzugsgebiet des unteren Weiße-Elster-Tales. Arbeits- und Forschungsberichte zur sächsischen Bodendenkmalpflege 45, 61–96.
Tinapp, C., Stäuble, H., 2000. Auenentwicklung und Besiedlungsgeschichte im Tal der Weißen Elster südlich von Leipzig. Trierer Geographische Studien 23, 31–48.
Tinapp, C., Meller, H., Baumhauer, R., 2008. Holocene accumulation of colluvial and alluvial sediments in the Weiße Elster river valley in Saxony, Germany. Archaeometry 50, 696–709.
Tinapp, C., Heinrich, S., Herbig, C., Schneider, B., Stäuble, H., Ahlrichs, J. & H. von Suchodoletz (2019): Holocene floodplain evolution in a Central European loess landscape – geoarchaeological investigations of the lower Pleiße valley in NW-Saxony. E & G – Quaternary Science Journal 68, 95–105.
Tinapp, C., Selzer, J., Döhlert-Albani, N., Fischer, B., Heinrich, S., Herbig, C., Kreienbrink, F., Lauer, T., Schneider, B., Stäuble, H., 2023. Late Weichselian–Holocene valley development of the Elbe valley near Dresden - linking sedimentation, soil formation and archaeology. E & G Quaternary Science Journal 72, 95–111.
TLB, 1993. Geological Map of Thuringia 1:25,000, Sheet Osterfeld. Thüringer Landesanstalt für Bodenforschung, Weimar.
von Suchodoletz, H., Faust, D., 2018. Late Quaternary fluvial dynamics and landscape evolution at the lower Shulaveris Ghele River (southern Caucasus). Quat. Res. 89, 254–269.
von Suchodoletz, H., Pohle, M., Khosravichenar, A., Ulrich, M., Hein, M., Tinapp, C., Schultz, J., Ballasus, H., Veit, U., Ettel, P., Werther, L., Zielhofer, C., Werban, U., 2022. The fluvial architecture of buried floodplain sediments of the Weiße Elster River (Germany) revealed by a novel method combination of core drillings with 2D and 3D geophysical measurements. Earth Surf. Process. Landf. 47, 955–976.
von Suchodoletz, H., van Meer, M., Kühn, P., Wiedner, K., Schunke, T., Reimann, T., 2023. Deciphering timing and rates of Central German Chernozem/Phaeozem formation through high resolution single-grain luminescence dating. Nat. Sci. Rep. 13, 4769.
Walker, M., Gibbard, P., Head, M.J., Berkelhammer, M., Björck, S., Cheng, H., Cwynar, L. C., Fisher, D., Gkinis, V., Long, A., Lowe, J., Newnham, R., Rasmussen, S.O., Weiss, H., 2019. Formal subdivision of the Holocene Series/Epoch: a summary. J. Geol. Soc. India 93, 135–141.
Wennrich, V., Wagner, B., Melles, M., Morgenstern, P., 2005. Late Glacial and Holocene history of former Salziger See, Central Germany, and its climatic and environmental implications. International Journal of Earth Sciences (Geologische Rundschau) 94, 275–284.
Wolf, D., Faust, D., 2013. Holocene sediment fluxes in a fragile loess landscape (Saxony, Germany). Catena 103, 87–102.
Zielhofer, C., 2022. Combined sediment grain size and silici-clastic element ratios represent the provenance signal – a reply to the comment of T. Matys Grygar (2022) on Ballasus et al. (2022). Sci. Total Environ. 846, 157210.